MacHydro

Effects of Forest Road Stream Crossings on Stream Temperature – Results of a Field Study in the Upper Oldman River Watershed

Prepared For:
fRI Research
1176 Switzer Dr.
Hinton, AB, T7V 1V3

Prepared By:
MacDonald Hydrology Consultants Ltd.
4262 Hilltop Cres.
Cranbrook, BC, V1C 6W3

Effects of Forest Road Stream Crossings on Stream Temperature – Results of a Field Study in the Upper Oldman River Watershed

Version 3.0 - November 2025

Suggested Citation:
Moore, R.D., MacDonald, R.J., Spannier., S., Wicharuk, N., and Kissinger, B. Effects of Forest Road Stream Crossings on Stream Temperature – Results of a Field Study in the Upper Oldman River Watershed. Prepared for fRI Research. 2025. 74 pp.

MacDonald Hydrology Consultants Ltd.
4262 Hilltop Cres.
Cranbrook, BC V1C 6W3
APEGA: #15531
EGBC: # 1001758

Contents

List of Figures

List of Tables

1 Document Versions

Version	Date	Comment
V2.0	November 2025	Initial draft of document. Internally reviewed and reviewed by fRI.
V3.0	November 2025	Final draft of document. Internally reviewed and reviewed by fRI.

2 Executive Summary

Stream temperature governs aquatic ecosystem function. Although there has been extensive research on the effects of land use on thermal regimes in lotic systems, little is known about the effect of forestry road crossings on stream temperature. Understanding these effects is important for managing watersheds along the eastern slopes of Alberta, where numerous streams are designated as critical for native trout. This study applied a spatial comparison - downstream (SCD) design to evaluate the effect of forestry road crossings on stream temperature in the headwaters of the Oldman River watershed.

Field work took place during the summer of 2024 and covered a range of stream sizes across the upper Oldman and Crowsnest watersheds. The SCD design used loggers positioned upstream and downstream of forestry road crossings, with five loggers per site. The upstream reference loggers suggested streams sampled warm by less than 0.4 °C in the absence of riparian disturbance (i.e. crossings). Where crossings were present, the largest effect was observed in maximum daily stream temperature. A key finding of this work is that the effects of road crossings on stream temperature were spatially variable with smaller catchment (<10 km^2) and stream sizes (< 3 m wide) being the most responsive.

Thermal changes observed here do not fall outside the range of tolerances for westslope trout or bull trout. Additionally, small streams like those responding to road crossings are suggested to have lower probability of native trout presence. However, these streams could still support populations by providing food and other resources. It is also possible that these streams provide important rearing or refuge habitats for young fish. These types of questions and the implications of changes in thermal conditions in response to road crossings will be explored in future work.

3 Introduction

Water temperature (T_w) is an important control on a range of biogeochemical, biological and ecological processes in aquatic systems (Webb et al., 2008). Decades of research in a range of forest ecosystems, as reviewed by Moore et al. (2005a) and Moore and MacDonald (2024), have demonstrated that reductions in riparian shade by logging, vegetation management or natural disturbance result in summertime warming by increasing the amount of solar radiation reaching the stream (Brown, 1969; Lynch et al., 1984; Isaak et al., 2010; Leach and Moore, 2010; Rex et al., 2012; Bladon et al., 2018; Raulerson et al., 2020; Leach et al., 2022). Post-logging stream warming has historically been of concern in relation to the potential degradation of thermally suitable habitat for cool and cold-water species such as salmonids (e.g., Cunningham et al., 2023). Retention of forested riparian buffer strips along streams within a cutblock is an effective approach to reduce post-harvest stream warming by maintaining stream shading (e.g., Gomi et al., 2006; Groom et al., 2011; Bladon et al., 2016). Studies have used a range of methodologies, ranging from observational studies based on spatial comparison approaches to more rigorous experimental studies employing before-after/control-impact (BACI) designs (Moore and MacDonald, 2024).

Road construction in forested landscapes involves clearing a linear strip of forest. Crossings can impact the biotic environment by increasing sedimentation causing loss of interstitial substrate spaces (Kemp et al., 2011), impact carbon transfer through the removal of vegetation (Tabacchi et al., 2000), create barriers to movement (Park et al., 2008; Diebel et al., 2015), and increase angling pressure (Hunt et al., 2011). Road crossings can expose the water surface to increased solar radiation, with the potential to cause stream warming. For these reasons, road crossings have been identified as a potential threat to aquatic organisms.

In the province of Alberta, Canada, three native salmonid species have been federally listed as Species-at-Risk (Athabasca rainbow trout *Oncorhynchus mykiss*, bull trout *Salvelinus confluentus*, and westslope cutthroat trout *Oncorhynchus lewsii*) due to cumulative effects which include those caused by road crossings (COSEWIC, 2016; Fisheries and Oceans Canada, 2020a, 2020b). Three species are all cold-water stenotherms that exist in cold and low productivity headwater streams (Nelson and Paetz, 1992). Increased water temperatures due to climate change and habitat loss (including road crossings) have been deemed a threat to these species (Isaak et al., 2012). As a result, critical habitats have been designated throughout their distributions and are protected under the Species At Risk Act (SARA). Critical habitats are defined as having sufficient flow of cold, clear water, and food availability for all life stage processes necessary for species survival. Although riparian processes are well understood (Naiman and Decamps, 1997), little research has focused on the thermal effects of roads and their rights-of-way.

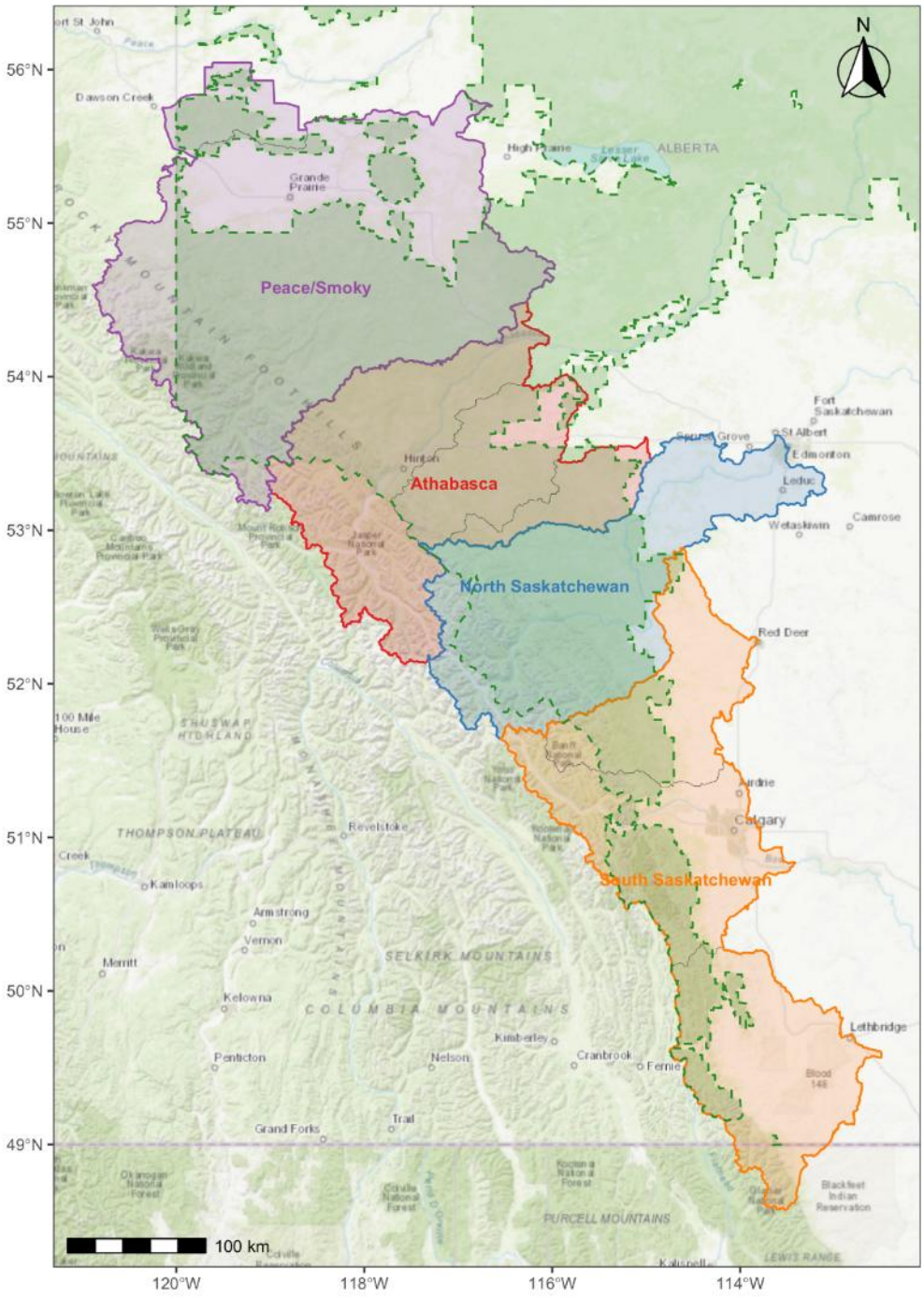

Figure 1 The headwater forested regions of the four major drainage basins in Alberta where forestry operations occur.

This research focuses on understanding road crossing effects on thermal regimes within the forested headwater regions of Alberta, Canada (Figure 1). This report describes results of a field study focused on quantifying the thermal effects of forest road stream crossings in the headwaters of the Oldman River watershed within the South Saskatchewan River Basin, Alberta, during summer and autumn of 2024. The report begins with a review of existing studies on the effects of road crossing on stream temperature and fish habitats more broadly, then focuses on the methods and results of the field study.

3.1 Literature Review

As can be seen in Table 1, all but one of the existing studies were based on "spatial comparison - downstream" designs, which involve comparing temperatures measured upstream and downstream of a road right-of-way with no pre-disturbance data. As discussed by Moore and MacDonald (2024), these studies cannot provide robust estimates of the effect of the right-of-way on stream temperature because there is no information regarding what downstream temperature changes would have been in the absence of the right-of-way clearing. However, a temperature change of 7 °C over 46 m and 5 °C over 30 m, as documented by Brown et al. (1971) and Herunter et al. (2003), respectively, are greater than typical natural downstream warming rates as shown in figures by Dent et al. (2008) and Arismendi and Groom (2019), for example. Further, such changes are not out of line with estimates of the effects of clearcut harvesting with no buffers (see, e.g., Moore et al., 2005a; Gomi et al., 2006).

Table 1 Summary of studies of road effects on stream temperature. Studies are arranged roughly in descending order of relevance to conditions in Alberta. Under study design, "SCD" indicates spatial comparison - downstream and "SCM" indicates spatial comparison- multi-stream. For the temperature metrics, "MWAT" is the maximum value of a seven-day running average of mean daily air temperature, and TDS and TUS are the temperatures measured upstream and downstream of the right-of-way clearing, respectively.

Location	Study design	Response variable	Result	Reference
North central BC	SCD	Maximum T_{DS} - T_{US}	Up to 5 °C change over a 30 m right-of-way	Herunter *et al.* (2003)
Central BC	SCM	MWAT	Bayesian regression indicated a 6-in-10 chance that MWAT would increase by 1.25°C for a road density of 2 km/km^2 of catchment area and 3.25°C for a road density of 4 km/km^2	Nelitz *et al.* (2007)
Oregon	SCD	Maximum T_{DS} - T_{US}	Increase of 7 °C in a 46 m reach that was completely cleared of vegetation during road construction	Brown *et al.* (1971)
Virginia Piedmont	SCD	Mean of T_{DS} - T_{US} spot measurements	Mean difference of 0.9°C for culvert and ford crossing, 0.4 to 0.5° for bridge and pole crossings	Aust *et al.* (2011)

New Brunswick	SCD	Mean daily T	Following replacement of two closed culverts with open-bottom culverts, longitudinal temperature patterns were inferred to be most responsive to removal of riparian vegetation and an old sediment pond	Caissie and Smith (2022)

In contrast to the studies that compared temperatures measured upstream and downstream of a road right-of-way, Nelitz et al. (2007) monitored stream temperature at several locations and then related the Maximum Weekly Average Temperature metric to measures of road density for the upstream catchment area.

While road rights-of-way are like harvest units in that they involve the removal of forest cover and thus expose a stream to increased incident solar radiation, they have some distinctive features that may influence their thermal impact. A major distinctive feature is that, whereas most jurisdictions require retention of forested riparian buffer strips along fish-bearing streams (at least above a certain width), road rights-of-way can impact all types and sizes of stream. This means that stream warming could be introduced throughout a stream network, and not just in unbuffered or poorly buffered headwater reaches. Drawing upon the work of Coats and Jackson (2020), larger streams lower down in the stream network are likely to warm less rapidly within an opening than smaller, headwater streams, but are also likely to cool less rapidly after flowing back into undisturbed forest.

Another difference is that the crossing structure would shade at least part of the stream's length, particularly for culverts. The crossing structure would also influence hydraulics and interactions with the substrate. For example, open-bottomed culverts and bridges would allow for hyporheic exchange with the substrate, whereas structures like corrugated metal pipe culverts would not (Caissie and Smith, 2022).

The roadbed and the associated drainage features such as ditches influence local hydrology. For example, during snowmelt and rain events, subsurface flow upstream of the road and overland flow generated by the road surface could be intercepted by the roadbed and ditch and diverted into the stream reach. Herunter et al. (2003) noted that ditch flow was observed mainly during snowmelt in April at sites in north central British Columbia, at which time the temperature of the ditch water was like that of the stream, and thus had minimal thermal impact. The first author of this report (RDM) observed road runoff entering streams during intense summer rain events at the same site as studied by Herunter et al. (2003). The stream water became noticeably turbid, and there could have been a short-lived temperature impact, depending on the difference in temperature between the road runoff and the stream water.

In addition to effects on stormflow, roads could potentially influence baseflow by diverting subsurface flow or intercepting flow from springs. Herunter et al. (2003) speculated that diversion of subsurface flow may have reduced relatively cool groundwater discharge into the stream within the right-of-way, which in turn would have enhanced the warming by increased solar radiation during summer.

4 Methods

4.1 Study Design

While before-after/control impact (BACI) designs are generally considered the most rigorous empirical approach to quantifying effects of forestry on stream temperature (Moore and MacDonald, 2024), they are challenging to implement because they require monitoring at multiple sites, all of which should be initially free of disturbance, for multiple years both before and after a forestry treatment has been executed. As an alternative, this study employed a replicated spatial comparison - downstream (SCD) design with an upstream reference segment at each site.

The design involved monitoring stream temperature at up to five locations at each stream crossing site, two upstream of the road and two or three downstream (Figure 2). While the goal was to install five loggers at each site, installation of a fifth at some sites was not feasible due to the presence of tributaries or confluences. For ease of reference, these logger locations are numbered from 1 to 5 from upstream to downstream. The term "reach" is used to refer to the length of stream bounded by the loggers 1 and 5 (or 1 and 4 at sites lacking the fifth logger), while "segment" is used to refer to the length of stream between two loggers.

Figure 2 Example showing locations of stream temperature loggers for the Oldman Rd km 6 site.

Loggers 2 and 3 were located at the upper and lower boundaries of the right-of-way, respectively. Logger 2 was typically located some distance upstream of the boundary to minimize the influence of

solar radiation penetrating into the forest upstream of the right-of-way. The distance was up to around 10 m and depended on a subjective in-field interpretation of stream orientation and vegetation characteristics.

Logger 1 was located a nominal distance of d_{ROW} upstream of logger 2, where d_{ROW} is the distance along the stream between the upper and lower boundaries of the right-of-way. Logger 4 was located a nominal distance of d_{ROW} downstream of logger 3, and logger 5 was installed the same distance downstream of logger 4. The actual distances between loggers deviated from d_{ROW} due to the need to find suitable locations in the channel in which to install the loggers – i.e., each logger should be in a part of the channel that is sufficiently deep to minimize the risk of de-watering during low-flow conditions and yet should remain connected to the main flow rather than becoming an isolated pool.

The segment between loggers 1 and 2 was intended to serve as an unimpacted reference for estimating "natural" downstream temperature variations. Loggers 4 and 5 were intended to quantify the downstream persistence of warming that occurred within the right-of-way.

4.2 Site selection

The initial intention was to use GIS analysis to generate a sampling frame of stream crossings and then to sample sites from that frame using a stratified random approach. However, field inspection revealed that many stream crossing sites were unsuitable, typically due to a lack of a well-shaded reference segment upstream of the crossing. As a consequence, site selection involved driving along forest roads in the Crowsnest Pass area and inspecting each crossing site encountered.

Site selection criteria ultimately included the following:

1. existence of a well-shaded upstream reference segment
2. existence of well-shaded segments downstream of the right-of-way
3. lack of tributaries or notable spring discharge within the study reach

Due to the challenges in finding suitable sites, criterion (2) was relaxed at some sites. In addition, a number of sites did not support installation of logger 5 – for example, due to bifurcation or a confluence with another stream a short distance downstream of logger 4.

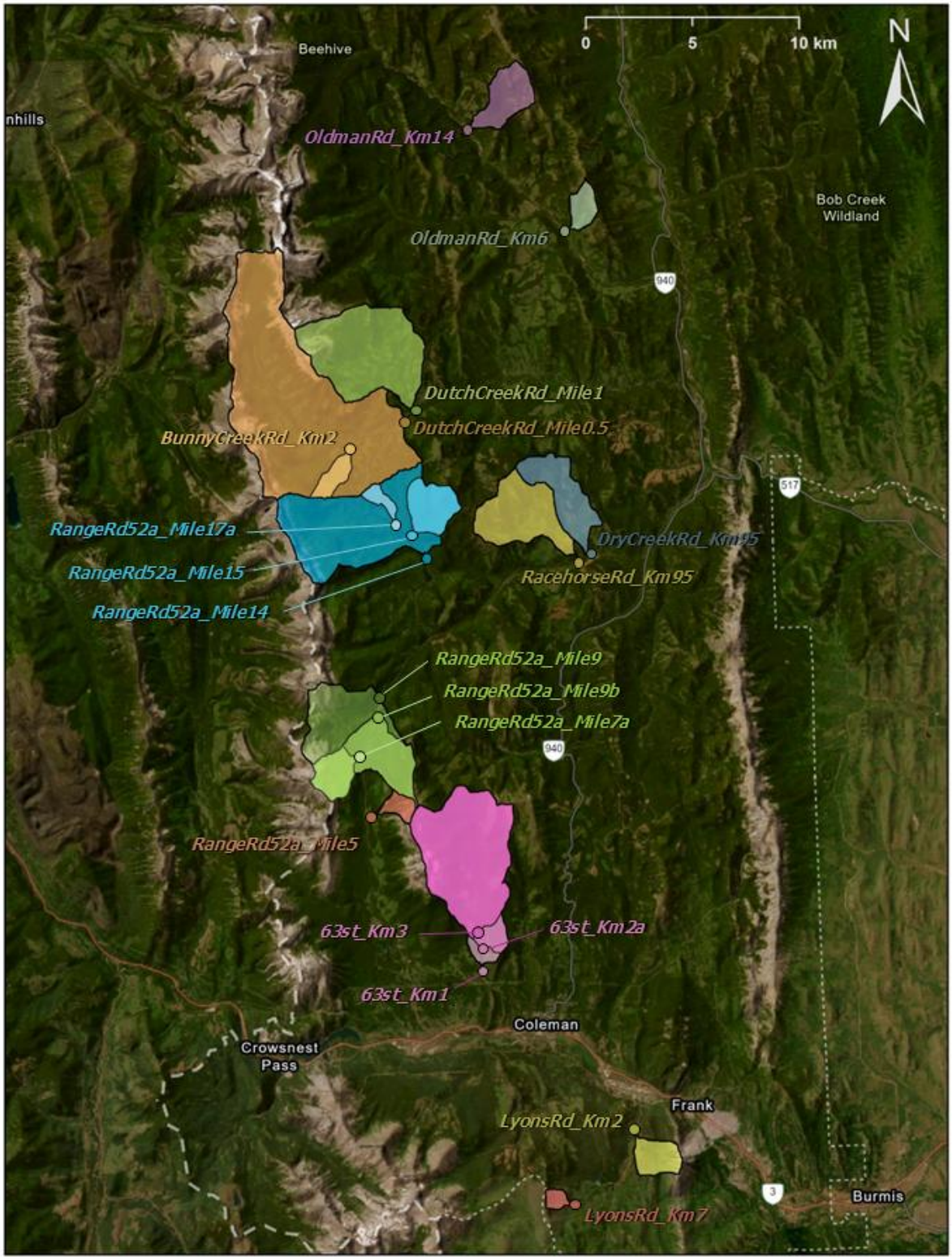

Figure 3 Watershed areas for each of the stream crossings.

As seen in Figure 3, the sample of sites spans a range of stream sizes, with upstream catchment areas ranging from about 0.9 km^2 to 55 km^2 and lengths of exposed channel within the right-of-way ranging from 20 m to 70 m. The relationship between bankfull width and catchment area is roughly linear on the log-log plot, consistent with a power-law relationship (Figure 4).

Seven sites had culverts and the remainder bridges. Bridges dominated sites with catchment areas greater than about 10 km^2, whereas both bridges and culverts were represented at sites with smaller catchment areas.

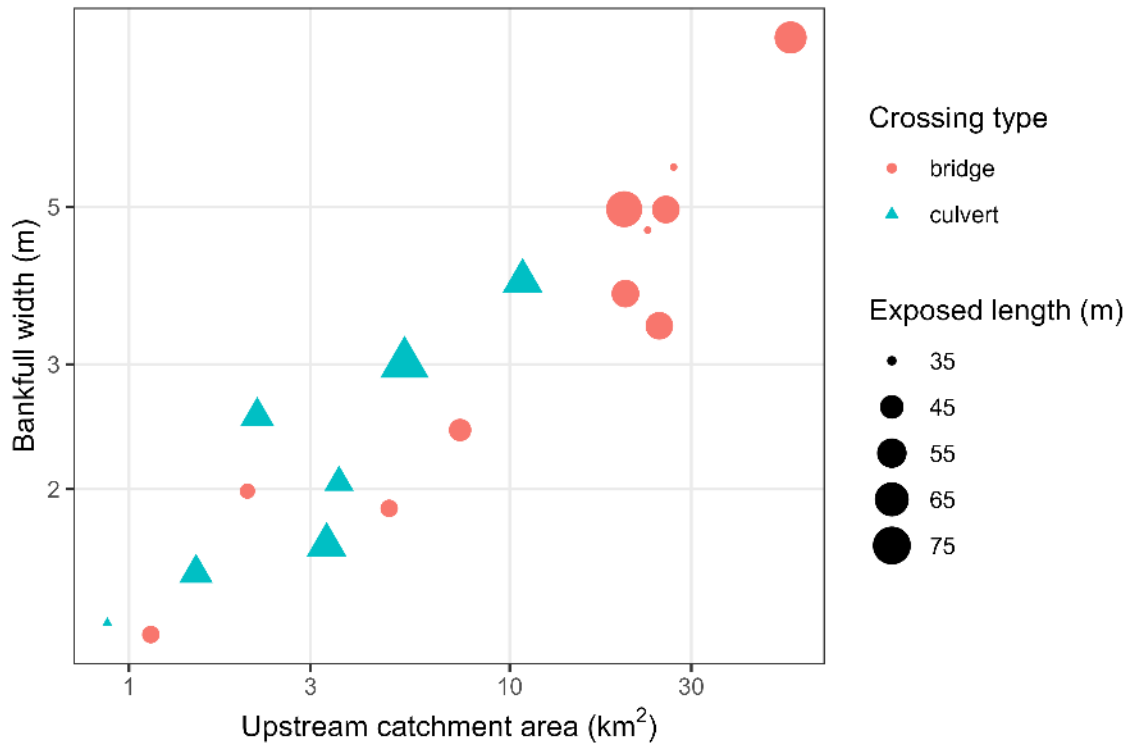

Figure 4 Summary of site characteristics, including catchment area upstream of the road crossing, mean bankfull width along the entire reach, exposed length of stream within the right-of-way, and crossing type. Both x and y axes are logarithmic.

4.3 Electrical conductivity and manual stream temperature measurements

During each site visit, electrical conductivity (EC) and stream temperature measurements were made at each temperature logger to provide an indication of groundwater discharge. Measurements were made using the probes built into a Sommer Tracer System TQ-S unit. As pointed out by Moore *et al.* (2008), downstream changes in EC and temperature, especially when abrupt, are usually diagnostic of groundwater discharge. Groundwater discharge typically results in cooling on warm summer days, while EC can increase or decrease, depending on whether the EC of groundwater is higher or lower than that of stream water (Story *et al.*, 2003).

4.4 Stream temperature

Stream temperature was recorded using Onset TidbiT loggers, which have a stated accuracy of ± 0.2 °C. Based on this accuracy and assuming a worst-case scenario, the temperature difference between two loggers would have an accuracy of ± 0.4 °C.

Temperatures were logged every 15 minutes. At some sites, loggers were housed in a white PVC cap that was attached to a length of rebar that was driven into the stream bed. At others, the loggers were in lengths of white PVC pipe that were attached to concrete weights. In both cases, loggers were installed at locations within the stream that were judged to be deep enough not to de-water under low-flow conditions but also to remain influenced by flowing water – i.e., not in a stagnant pool.

Logger installation began on 2024-06-10 and was completed by 2024-06-21. Loggers were removed between 2024-10-14 and 2024-10-25. At the end of the field season, temperature loggers were downloaded upon removal. The data were examined using interactive time series graphs generated using the 'plotly' application within an R script (Sievert, 2020) following Callahan and Moore (2025). These plots allowed comparison among records and also provided the ability to zoom in and out along both the time and temperature axes. As Sowder and Steel (2012) emphasized, visual examination is generally more effective than automated data cleaning procedures.

During each site visit, manual water temperature measurements were made using the temperature probe built into the Sommer Tracer System TQ-S probe, which has an operating range of 0 - 60 °C a stated accuracy of 0.02 °C. For each manual measurement, the closest-in-time recorded value was extracted and the two values compared as a check for drift or other errors in the TidbiT sensors.

4.5 Weather data

Weather data were drawn from three stations as listed in Table 2. Daily weather observations for the Crowsnest weather station (WMO ID 71236) for the period 1994 to 2024 were used to provide a basis for placing the field season into a historical context.

Table 2 Locations of weather stations. ECCC is Environment and Climate Change Canada.

Station name	Longitude (°W)	Latitude (°N)	Elevation (m)	Operator
Crowsnest	114.4830	49.81738	1303	ECCC
South Racehorse Creek	114.4835	49.81676	1678	MacHydro
Livingstone Gap	114.3827	49.87930	1417	Province of Alberta

To provide more detailed data to support the analysis, a weather station was set up by MacHydro at South Racehorse Creek. This station used a Hobo data logger and Hobo sensors to record air temperature, relative humidity, rainfall, atmospheric pressure, wind speed and direction, and incident global solar radiation. Dewpoint temperature was computed based on recorded air temperature and relative humidity. The station ran from 2024-06-29 to 2024-10-31, and recorded data every 15 minutes.

To extend the South Racehorse Creek weather record back to 2024-06-01, regression equations were fit between rainfall, air temperature and dewpoint temperature at South Racehorse Creek and the corresponding variables recorded hourly at the Livingstone Gap station.

4.6 Stream discharge

4.6.1 Water Survey of Canada data

Streamflow data recorded at two stations operated by Water Survey of Canada (WSC) were accessed using functions in the **tidyhydat** R package (Albers, 2017) for the period up to and including the year 2022. Station information is provided in Table 3. Data for the 2024 field season have not undergone final approval, so provisional data were acquired via the WSC web site. These data were provided with a time interval of 5 minutes and were aggregated to daily means.

Table 3 Characteristics of Water Survey of Canada gauging stations.

Station number	Station name	Latitude (°N)	Longitude (°W)	Area (km²)
05AA008	Crowsnest River at Frank	49.59732	114.4106	403
05AA027	Racehorse Creek Near the Mouth	49.83779	114.4206	218

4.6.2 Manual streamflow measurements

During each site visit, streamflow was measured toward the upstream and downstream ends of the reaches using slug injection of salt with a Sommer TQ-S system. Locations of the injection point and the electrical conductivity (EC) probes were selected to provide the best conditions for complete lateral mixing. A measured mass of salt was injected as a brine and the breakthrough curves were recorded until EC returned to the pre-injection background. Both probes were calibrated in the field following each measurement. Discharge calculations were conducted by the software application provided with the TQ-S system.

A nominal uncertainty in each measurement was estimated based on the difference in discharges computed from data for the two probes:

$$u_Q = 100\% \frac{|Q_1 - Q_2|}{0.5(Q_1 + Q_2)} \qquad (1)$$

where Q_1 and Q_2 are the discharges from each of the two EC probes. Because the standard deviation of a sample of two is equal to half the difference, Equation (*1*) provides a two-sigma estimate of relative uncertainty, which corresponds approximately to a 95% confidence interval.

4.6.3 3.6.3 Continuous estimates of streamflow at each site

Continuous estimates of streamflow were generated for each site by relating salt-dilution measurements to mean daily streamflow for that date as measured at each of the two WSC stations. The regression model took the following form:

$$f_i(t) = \frac{Q_i(t)}{Q_{wsc}(t)} = b_0 + b_1 Q_{wsc}(t) + e(t) \qquad (2)$$

where $Q_i(t)$ is the mean of the upstream and downstream discharge measurements at site i on day t (m^3s^{-1}), $Q_{wsc}(t)$ is the discharge at one of the Water Survey of Canada stations on day t, b_0 and b_1 are coefficients to be estimated using ordinary least squares regression, and $e(t)$ is the residual from the

fitted regression (m^3s^{-1}). Equation (2) was fit using data for each of the two WSC stations for all sites with at least three measurements, and the model with the lowest p-value selected for use if that p-value was less than $\alpha = 0.1$.

Time series of predicted discharge for each site were then computed as

$$\hat{Q}_i(t) = \hat{f}_i(t) Q_{wsc}(t) \qquad (3)$$

where $\hat{f}_i(t) = b_0 + b_1 Q_{wsc}(t)$. Prediction limits for $\hat{f}_i(t)$ for a confidence level of 68.3% (i.e., one sigma) were generated and applied in Equation (3) to indicate uncertainty.

For sites with only two streamflow measurements, or where neither regression was statistically significant at $\alpha = 0.1$, the mean and standard deviation of the fraction of site-measured discharge to recorded discharge were computed for each of the two WSC stations, and the WSC station associated with the lower standard deviation was used as the reference. Estimated streamflow was then calculated as the product of the mean fraction and the recorded discharge, and uncertainty was estimated as the product of the standard deviation of the two fractions and recorded discharge.

One site had only a single discharge measurement. The fraction of that measurement relative to the recorded discharge was used to estimate streamflow, and no uncertainty estimate was generated.

4.7 Channel and site characteristics

Stream bankfull width was measured at 5-m intervals along each reach, beginning at logger 1. The type of crossing structure (bridge vs culvert) was recorded and the upstream and downstream locations of the crossing structure were measured as distance downstream of logger 1.

4.8 Solar radiation

Above-stream solar radiation was computed using upward-looking hemispherical photographs taken at roughly 10-m intervals along each reach, beginning 5 m downstream of logger 1. The photos were taken with a Nikon DF camera.

4.8.1 Field protocol

At each photo location, the tripod was set up with legs extended once if possible, which set the height of the photo between 0.5 and 0.75 m above the stream surface. More leg extensions were used as needed in deeper water. The camera was leveled first by using the built-in bubble level on the tripod followed by checking the lens with a level placed on the lens cap.

The orientation of north from the camera location was determined by holding a compass sufficiently high above the camera to avoid the metal on the camera influencing the magnet. One worker then stood or sat directly north of the camera while holding a PVC pipe straight up so that its position in the image would indicate north. The other worker knelt beside the camera while operating it to avoid being in the photo.

Several photos were taken and then checked to make sure that north could be found in the photo and the photo looked properly exposed and representative of the canopy. The best photo taken at the location was chosen to be used for analysis.

This process continued at 10-m intervals downstream until a photo was within 10 m of the next temperature logger. The camera was then moved 5 m downstream of that logger and the process was repeated until the lowest logger (4 or 5) was reached. Each segment contained between 2 and 9 camera sites.

At sites with bridges, photographs were taken along the stream as described above so that the shading effect of the bridge was sampled by the photographs. At sites with culverts, photographs above the culvert were taken to represent total openness of the canopy through the crossing.

4.8.2 Photo processing

Following the field campaign, photos were first checked to confirm that the photo chosen in the field was of sufficient quality for determining gap fractions and estimating above-stream solar radiation. The chosen photo for each camera location was rotated in R based on user inputs until the north identifier in the photo was aligned with the top-middle of the photo (where a pointer was added to the digital image for reference). The photo was then cropped to remove additional blank space outside of the circular photo and flipped so that the clockwise azimuth segments aligned properly with east and west. The digital file containing the rotated photo was then saved to a folder.

Each photo was then processed using functions in the R **HemispheR** package (Chianucci and Macek, 2023). Each photo was first binarized using the Otsu method and visually checked. If needed, thresholding values were manually adjusted until the photo looked properly binarized. Gap fractions were then computed for cells defined by angular intervals of 5° for both azimuth and zenith. The gap fraction arrays for each camera location were then saved as a csv file.

Several photos contained areas of lens flare, which is not ideal. Wherever possible, photos with lens flare were replaced with another photo from the location that did not have lens flare or overexposure. Where photos could not be replaced, the photo was modified by changing the exposure, contrast, etc. around the overexposed area/lens flare. In this process, the goal was to darken the impacted canopy area to a point where thresholds could be properly chosen. In most cases the concerns were relatively small and all that needed to be removed was streaks from lens flare. Any photo where the issues could not effectively be removed were noted in an additional csv to be removed from the analysis if necessary. Photos for which lens flare impacted more than two sky dome cells that would not have been considered sky were considered as low quality.

4.8.3 Calculation of above-stream solar radiation

Measured solar radiation at the South Racehorse Creek weather station was partitioned into direct and diffuse components using the Erbs *et al.* (1982) formula. These values were combined with the gap fraction array for each camera location to compute time series of direct, diffuse and total above-stream solar radiation for each camera location following the equations described by Moore *et al.* (2005b) and Leach and Moore (2010). These 15-minute values were averaged each day between 09:00 and 15:00; this interval captures the main period of diurnal stream warming and thus should be relevant for daily mean and daily maximum stream temperatures. For each site and segment, the mean and standard error of the mean were computed, the latter to provide an indication of the uncertainty associated with sampling a relatively small number of locations in each segment.

A measure of the integrated input of solar radiation along each segment was computed as

$$SR_{int}(i,j,t) = L(i,j)SR(i,j,t) \qquad (4)$$

where $SR_{int}(i,j,t)$ is the integrated input for segment j at site i on day t (W m^{-1}), $L(i,j)$ is the length of the segment j at site i (m), and $SR(i,j,t)$ is the mean of the daily solar radiation estimates for segment j at site i (W m^{-2}). For crossings with culverts, the segment length used in Equation 4 excludes the culvert.

4.9 Data analysis

Scatterplots and time series graphs were generated as part of an initial stage of exploratory analyses to quantify the spatial and temporal variability of stream temperature and its relationships with air temperature and stream discharge. Time series of daily minima, means and maxima were generated for each logger at each site. Time series of downstream temperature changes for each segment were then computed from the minima, means and maxima.

The difference between temperatures for loggers 1 and 2 was assumed to provide an estimate of downstream temperature changes under undisturbed conditions as a reference to assess the influence of the right-of-way clearing on temperature changes between loggers 2 and 3. The validity of this assumption and its implications are addressed in the discussion. To explore the downstream persistence of the thermal impact of the right-of-way clearing, downstream temperature changes between loggers 3 and 4 and between loggers 3 and 5 were compared to the change from logger 2 to logger 3 (the segment containing the right-of-way).

5 Results

5.1 Overview of the study period

As seen in Figure 5, air temperature sustained high values, often near 30 °C, through July and into early August. Except for one day with almost 25 mm of rainfall, that period was relatively dry. In contrast, August experienced relatively frequent rainfall and lower air temperatures. Warm and dry conditions dominated the first half of September, followed by a shift back to wetter, cooler conditions. Except for a short-term increase in streamflow in mid-July, that month was dominated by a smooth streamflow recession at both stream gauges following the cessation of seasonal snowmelt. The hydrographs for both streams flattened in August, in part due to the regularly frequent rainfall events. Stream temperatures generally remained relatively high through July, and most sites experienced the highest daily maximum stream temperatures in early August, with somewhat lower temperatures dominating August and September.

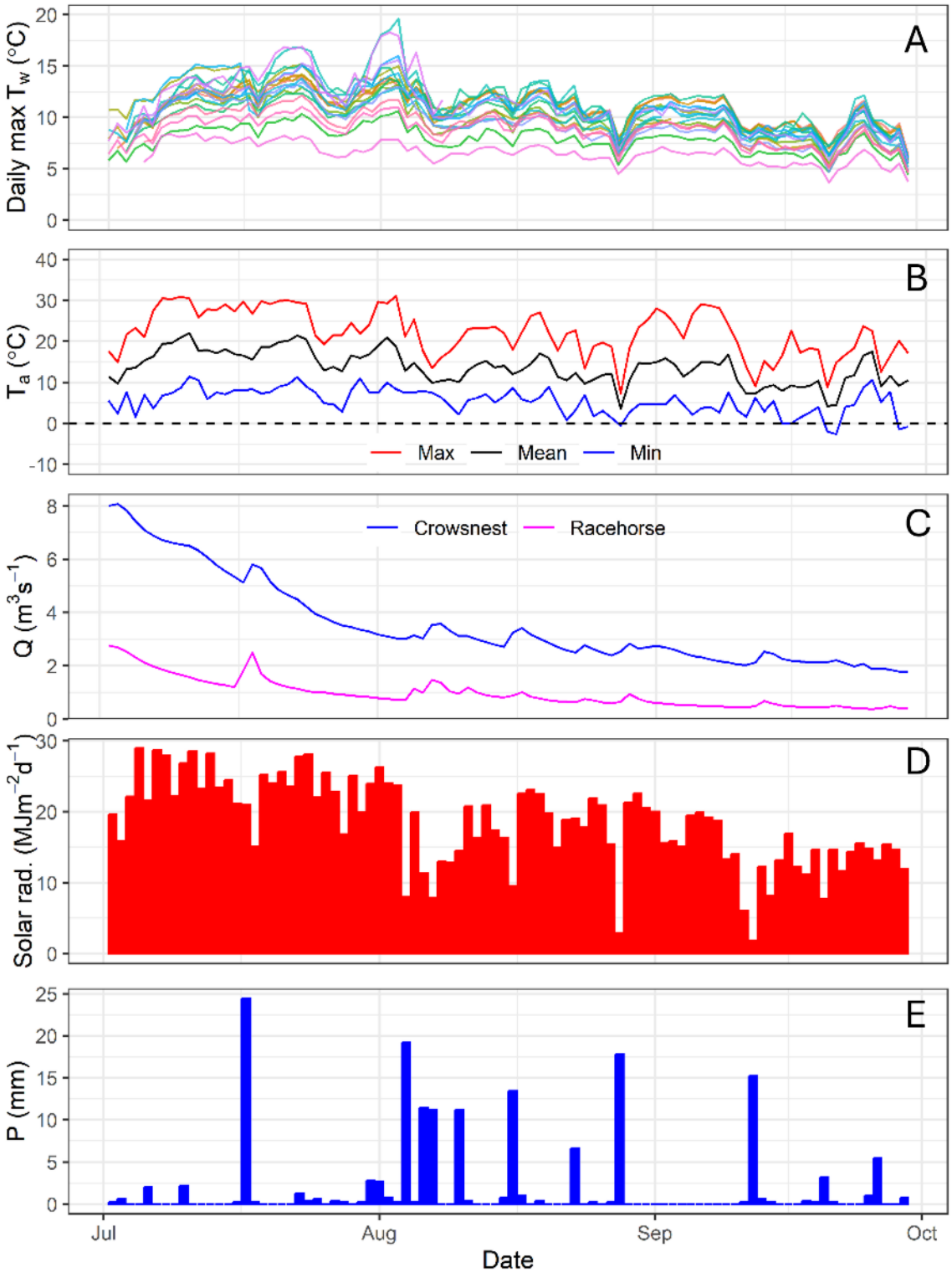

Figure 5 Hydrometeorological conditions during the study period. From top to bottom, the panes show (a) time series of daily maximum temperature at logger 3 for each site (distinguished by colour); (b) daily maximum, mean and minimum air temperature at the South Racehorse Creek weather station; (c) daily mean streamflow at the Crowsnest River and Racehorse Creek gauging stations; (d) daily global solar

radiation at the South Racehorse Creek weather station; and (e) daily total rainfall at the South Racehorse Creek weather station.

Daily maximum air temperature in 2024 varied substantially within the range of data for the period 1994 to 2023, approaching both the minimum and maximum values experienced as a function of date (Figure 6). An extended period of air temperatures around 30 °C dominated much of July and the first week of August. Streamflow at both Racehorse Creek and Crowsnest River were dominantly below the longer-term median by date through June and July, and close to the median for much of August (Figure 7).

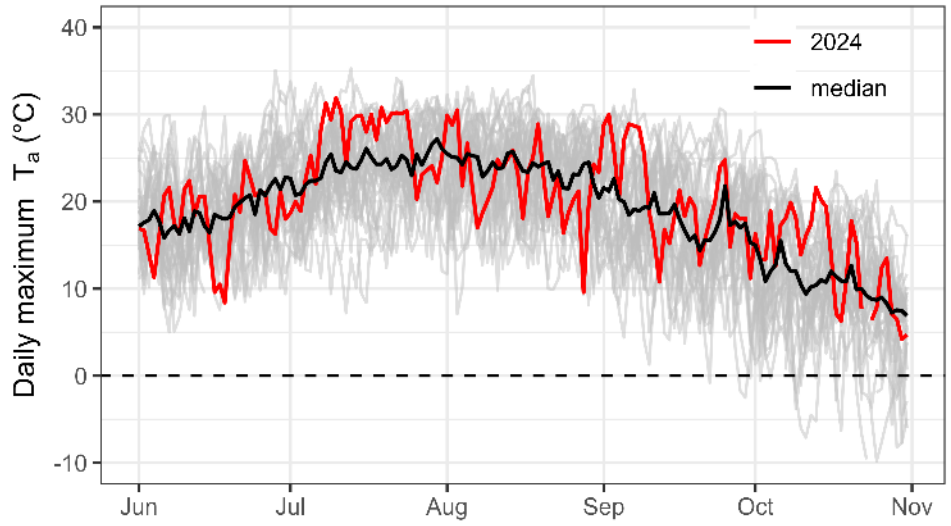

Figure 6 Daily maximum air temperatures recorded by date at the Environment and Climate Change Canada Crowsnest weather station. Each grey line represents a year from 1994 to 2023, the red line indicates the data for 2024, and the black line is the median by date.

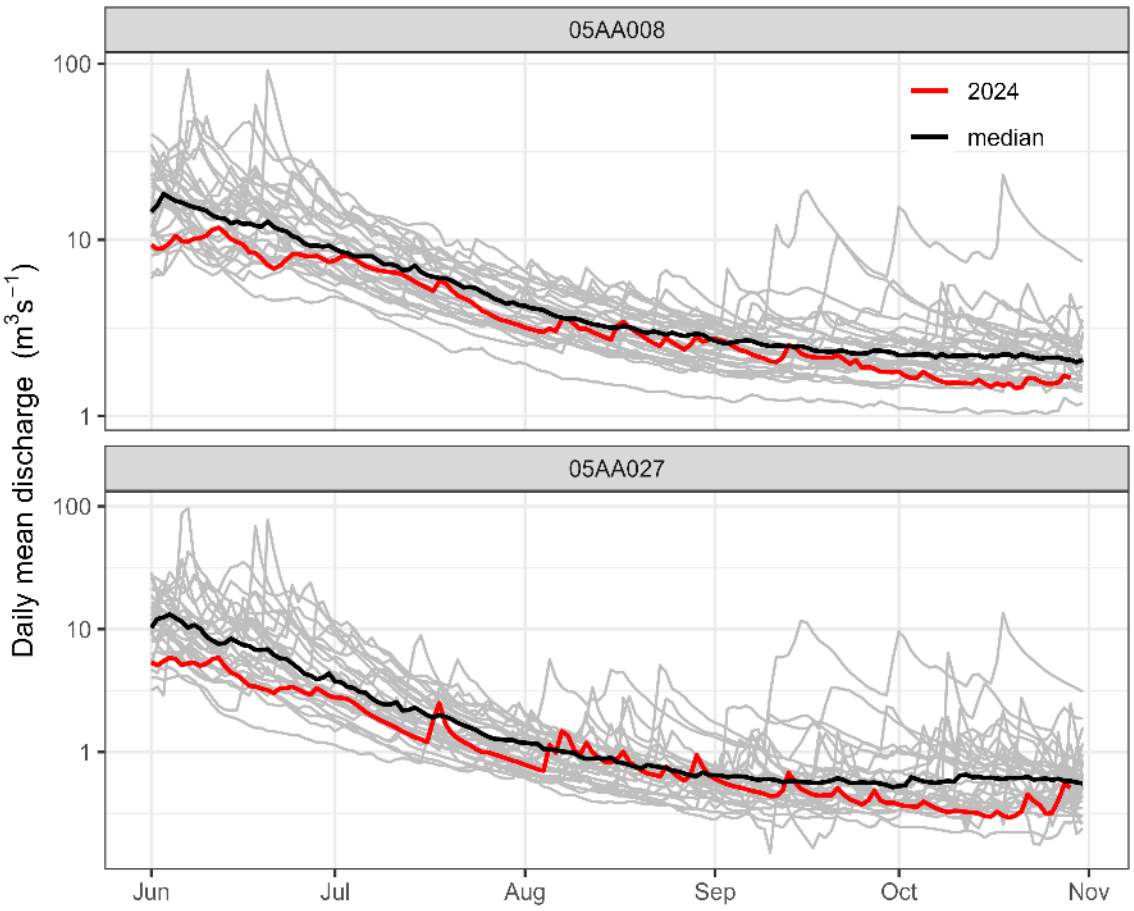

Figure 7 Daily mean stream discharge recorded by date at Crowsnest River (05AA027) and Racehorse Creek (05AA008) Water Survey of Canada gauging stations. Each grey line represents a year in the common period of record from 1966 to 2022, the red line indicates the data for 2024, and the black line is the median by date.

5.2 Streamflow measurements

As seen in Figure 8, there was generally good agreement between the discharges determined from the two EC probes, indicating that the assumption of complete lateral mixing of the salt tracer is reasonable. The uncertainty is less than ± 10% in all cases, and is mostly less than ± 5%.

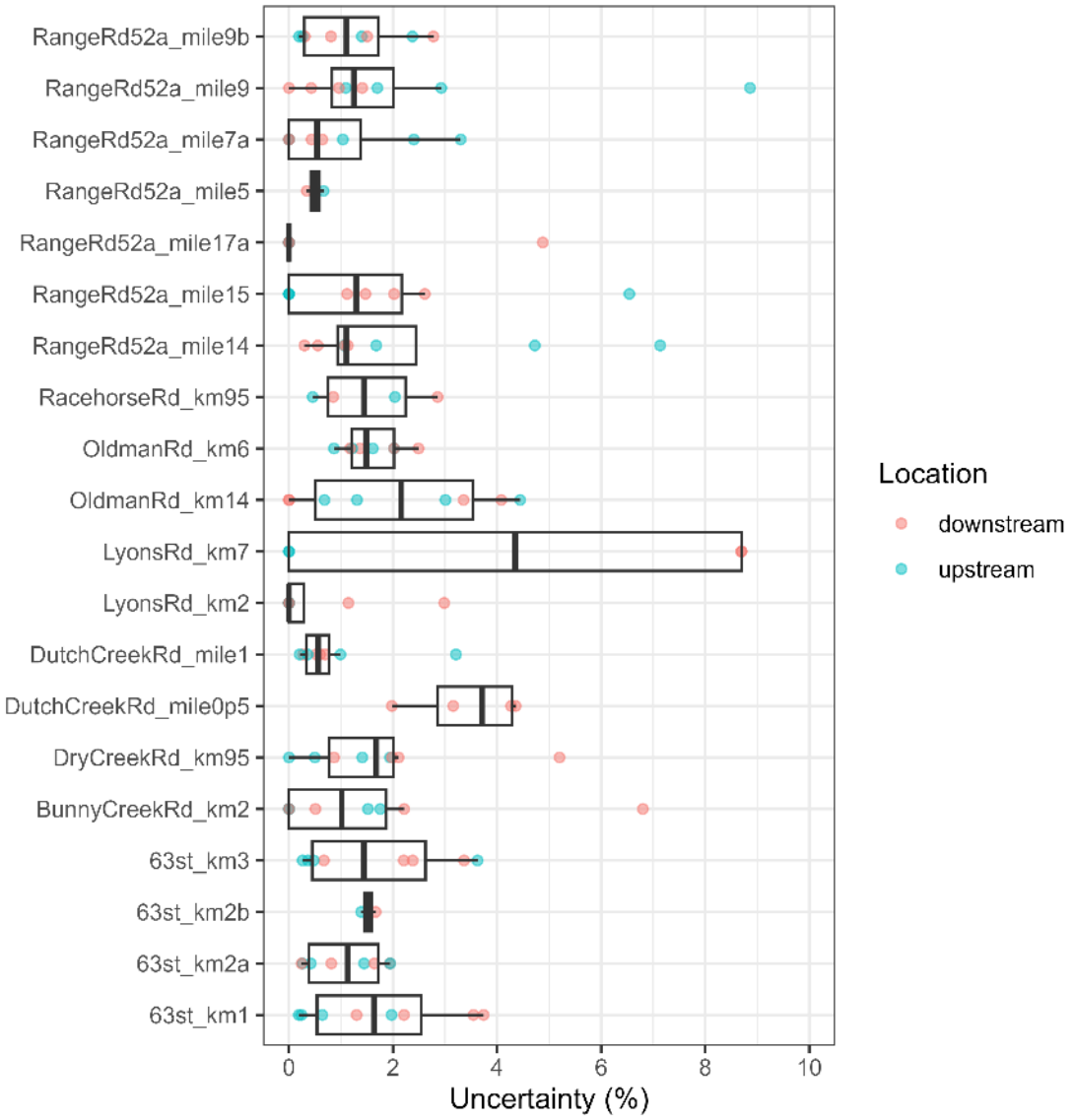

Figure 8 Estimated uncertainty in measured streamflow based on differences between the discharges determined using each EC probe. As explained in the text, the uncertainties correspond to two-sigma intervals.

As seen in Figure 9, measured streamflow at the sites generally followed a similar seasonal decline as recorded at the two WSC gauging stations. However, some sites apparently had a more marked response to rain events in August than is evident at the WSC gauges.

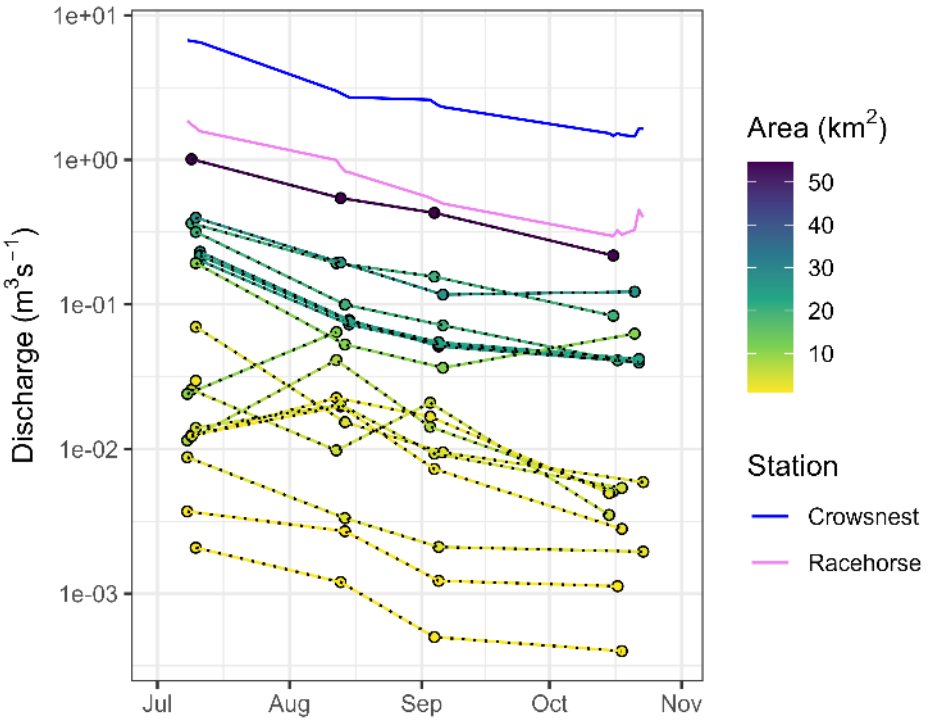

Figure 9 Streamflow as a function of date. Symbols connected by lines are the averages of upstream and downstream discharge measurements at each site, and the symbol and line colour indicate the upstream catchment area at the road crossing. Also shown are daily mean discharges at the Water Survey of Canada gauging stations on Crowsnest River and Racehorse Creek.

Figure 10 shows that some sites, such as RangeRd52a_mile7a, had reasonably strong relationships between the streamflow ratio and streamflow at a WSC gauge, but many did not. Hence, the estimated streamflow time series shown in Figure 11 should be considered rough indices of streamflow variability through the study period, especially for sites with wide prediction limits, such as DryCreekRoad_km95.

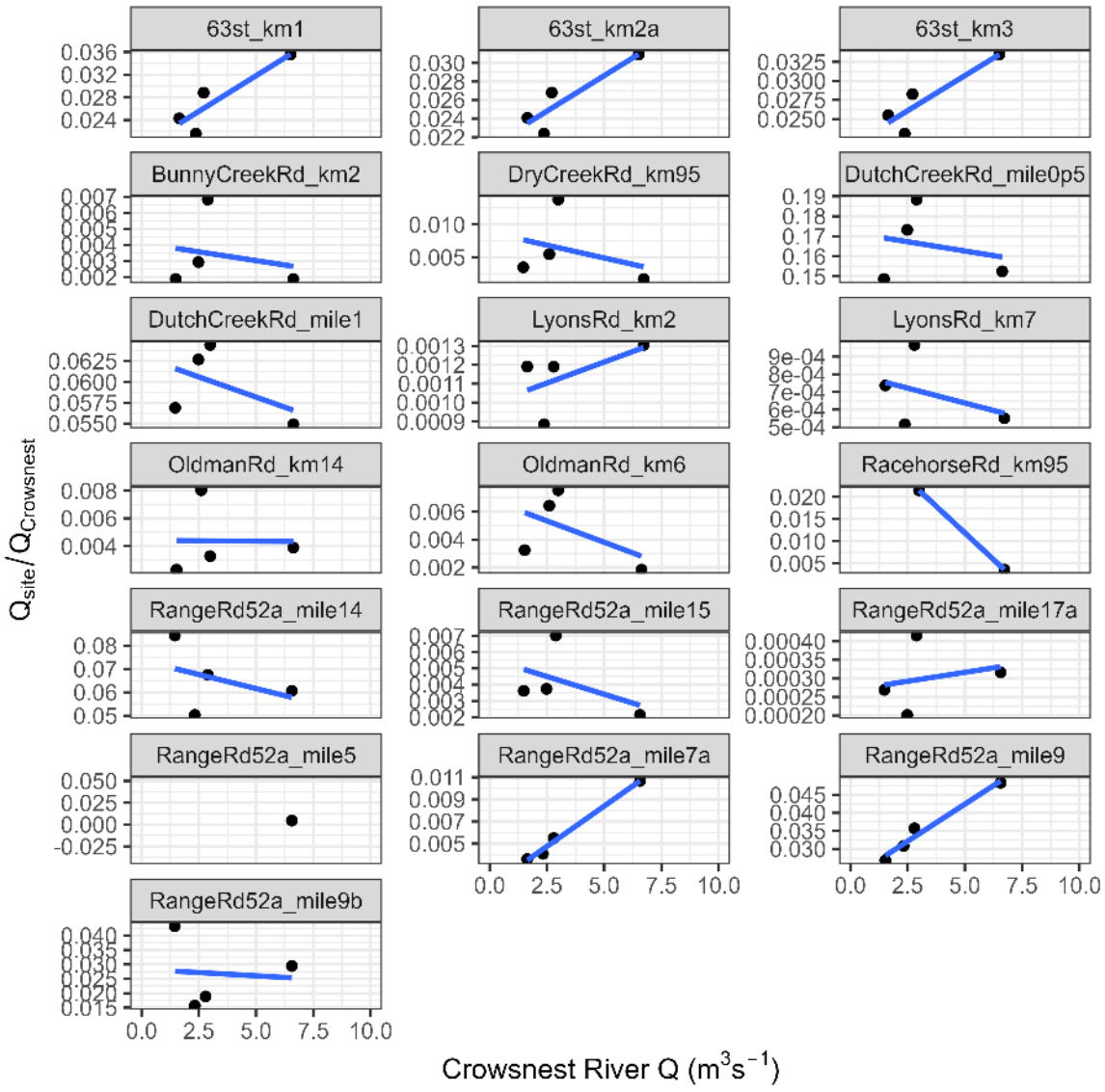

Figure 10 Ratios of streamflow measured at each site to streamflow recorded at Crowsnest River. The blue lines are best-fit linear regressions.

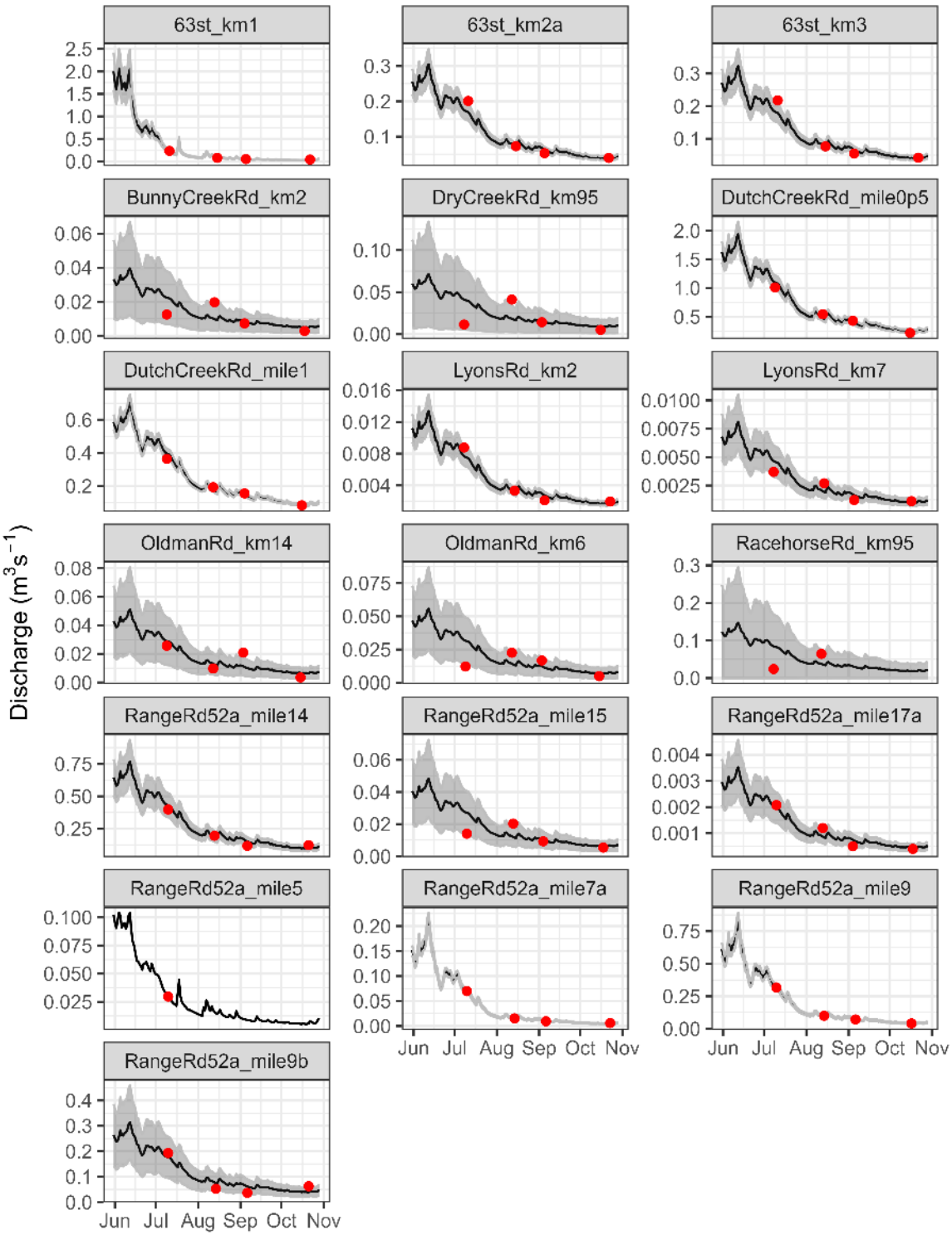

Figure 11 Time series of estimated streamflow at each site. The grey ribbons represent one-sigma uncertainty bounds based on prediction intervals around the regression relationships and the red symbols indicate the measured discharges.

5.3 Solar radiation

Figure 12 illustrates the standard error of the mean for the estimated above-stream solar radiation for each segment-day in relation to the mean. The standard error represents a one-sigma uncertainty in the mean that is associated purely with sampling variability, and is a function of both the within-segment variability and the sample size. As shown in the figure, the uncertainty associated with sampling variability often exceeds 50% of the mean.

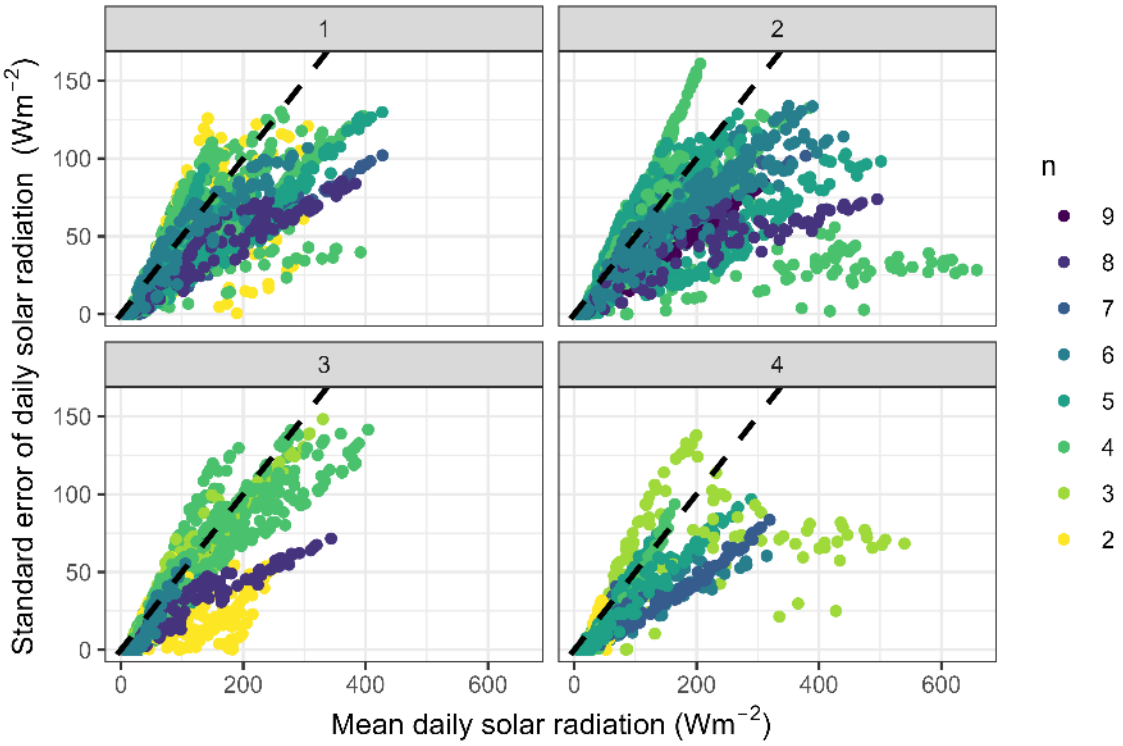

Figure 12 Standard error of the mean daily above-stream solar radiation for each segment as a function of the mean solar radiation. The dashed line indicates that the standard error is 50% of the mean for visual reference.

Figure 13 shows time series of estimated above-stream solar radiation for each segment and site. All segments and sites exhibited an overall seasonal decline, with shorter-term fluctuations related to varying cloud cover through time.

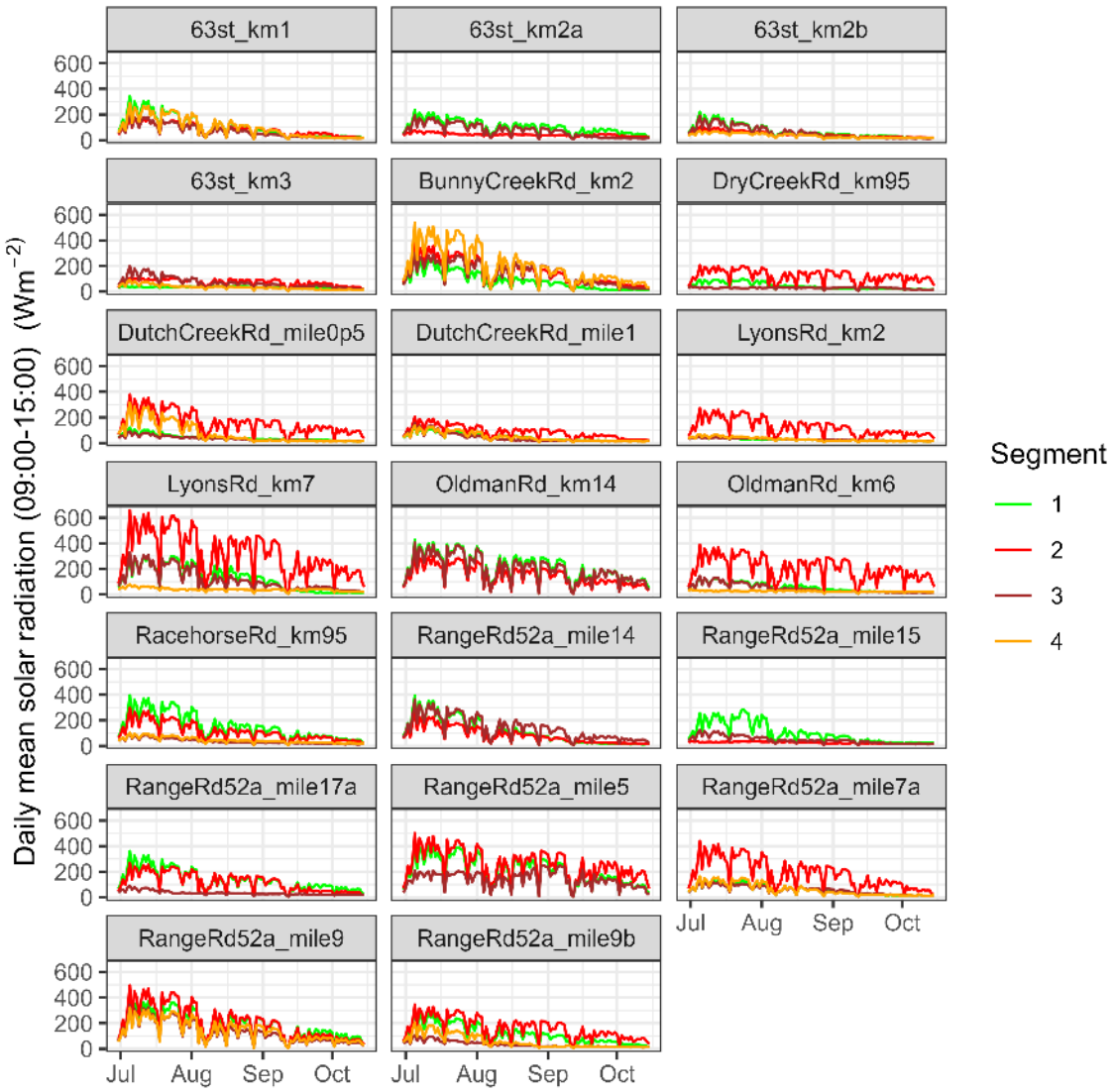

Figure 13 Time series of estimated above-stream solar radiation for each segment and site.

The contrasts among segments are illustrated more clearly in Figure 14. As can be seen, the contrasts between the right-of-way segment and the others were not always strong. At the 63st sites, the right-of-way remained relatively well shaded due to the relatively tall forest and east-west orientation of the stream. At Bunny Creek, the road ran roughly parallel to the stream except near the crossing itself, leading to a relative lack of shading in segment 4.

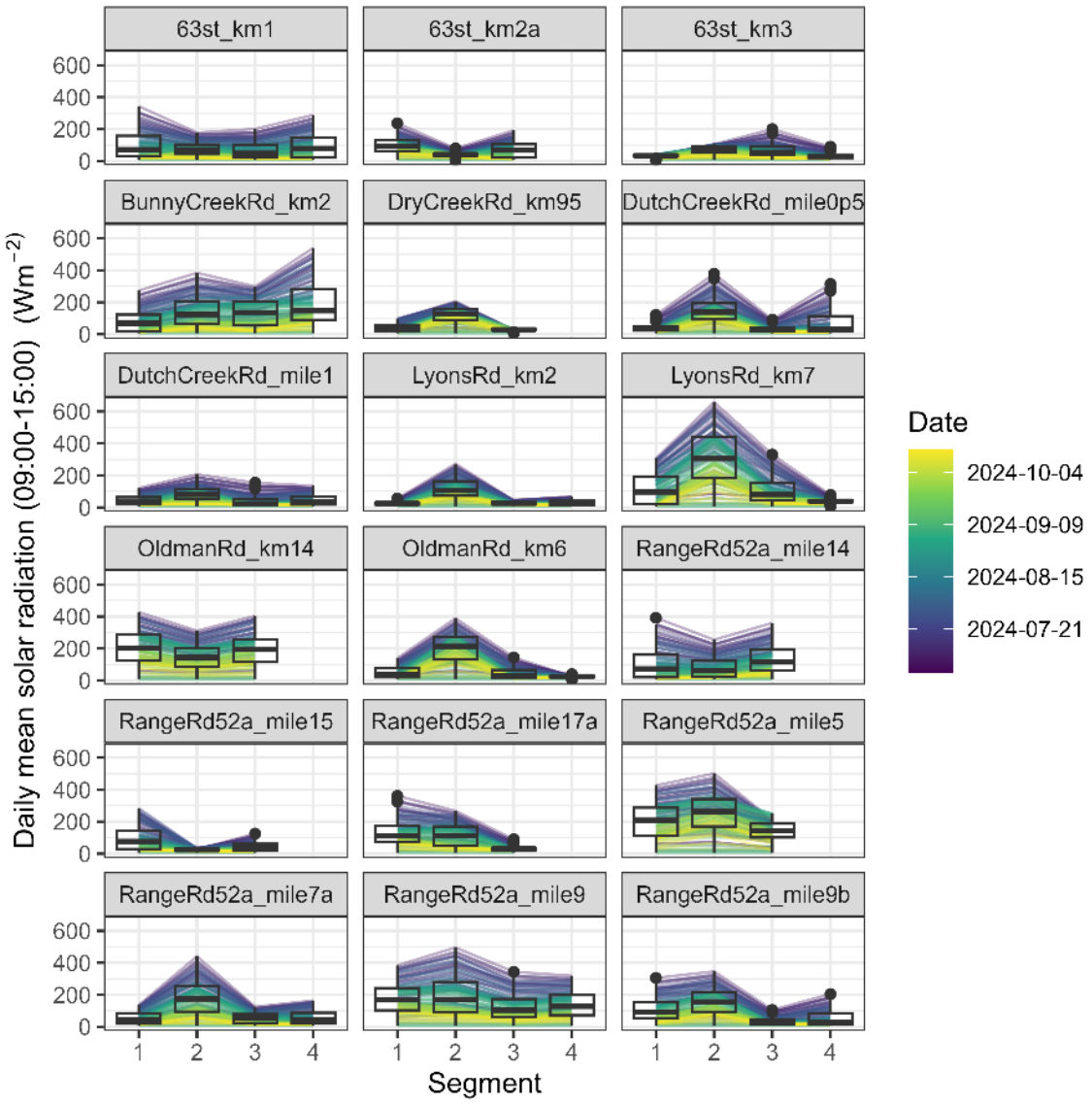

Figure 14 Boxplot of estimated above-stream solar radiation by segment for each site.

5.4 Occurrences of incomplete stream temperature data

Five sites ended up having incomplete temperature data for a variety of reasons. During a site visit on 2024-08-13, all loggers at RangeRd52a_mile5 were found to be de-watered, and examination of the temperature data suggested the de-watering began 2024-08-09.

At OldmanRiver_km14, logger 4 was dry or intermittently dry from 2024-07-29 to 2024-08-06, as evidenced by recorded temperatures similar to the recorded air temperature. Following precipitation that occurred from 2024-08-05 to 2024-08-07, temperatures returned to normal and logger 4 was in water at the site visit on 2024-08-12. Logger 4 was de-watered again from 2024-09-06 to the last site visit on 2024-10-15. During that site visit, the stream had little water flowing at the location of logger 4 and the logger itself was not in water.

At 63st_km2b, the stream was found to be entirely dry between logger 2 and the start of the crossing on the 2024-08-15 site visit, and logger 2 was out of water. Based on the temperature data, logger 5 was interpreted to be dry or intermittently dry starting 2024-07-21. Loggers 3 and 4 were dry or intermittently dry starting 2024-07-23. Logger 2 was dry or intermittently dry starting 2024-08-08. All loggers were removed from the site on 2024-09-05. Based on attempts to delineate the catchment for this site, it was found that this site was likely a side channel of McGillvray Creek.

At RangeRd52a_mile7a, logger 4 was dry or intermittently dry starting 2024-10-10 until removal at the last site visit on 2024-10-23. When the logger was removed it was covered in mud and partially out of the water. Diel temperature fluctuations were partially suppressed by water but were greater than at the other loggers at this site, and appeared to be following air temperature.

At RacehorseRd_km95, logger 2 and its casing were found to be missing at the 2024-08-12 site visit. It was assumed that the casing and logger were stolen. No other loggers appeared to have been tampered with. Due to the loss of Logger 2, field visits were stopped after 2024-08-08, but loggers were allowed to continue logging until 2024-10-15.

5.5 Comparison of manual spot and recorded stream temperature

As seen in Figure 15, manual spot temperatures and the nearest-in-time recorded values agreed to within $\pm$ 0.5 °C for all but one measurement. Overall, 87% of the paired measurements differed by less than $\pm$ 0.2 °C and 97% differed by less than $\pm$ 0.4 °C. These results confirm that none of the loggers appears to have experienced significant drift over the period of deployment in the field.

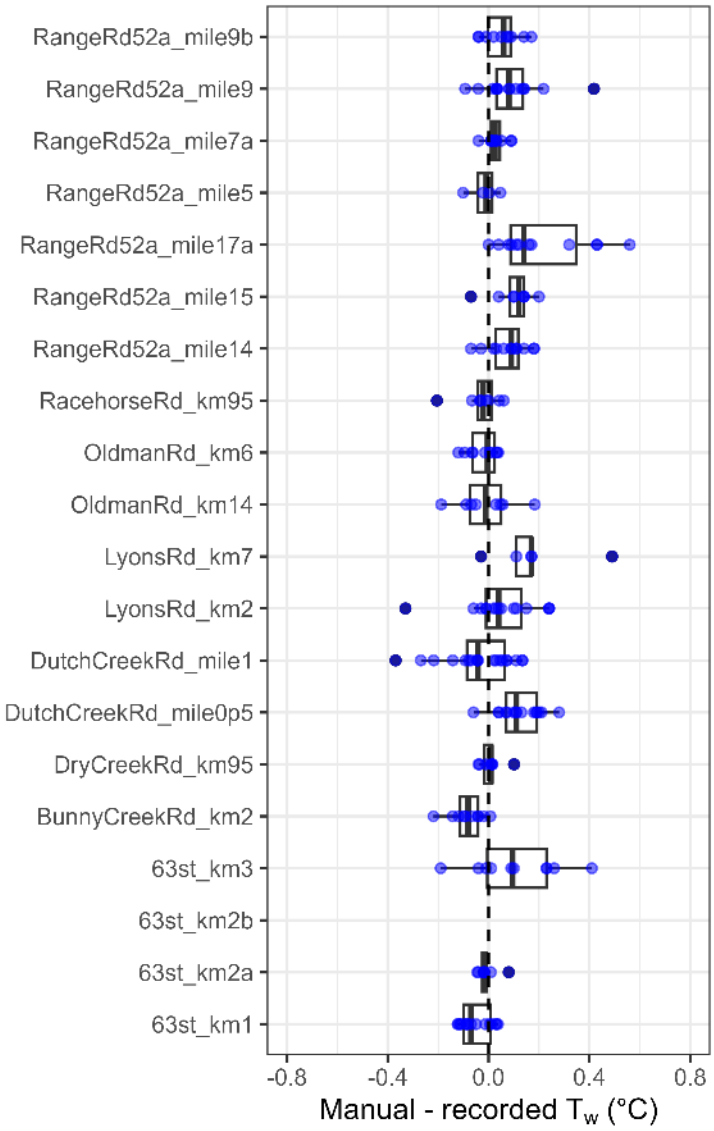

Figure 15 Differences between manual spot temperature measurements and the nearest-in-time recorded value by site.

5.6 Upstream-downstream streamflow measurements and electrical conductivity

As seen in Figure 16, most reaches were relatively neutral, with no marked increases or decreases in streamflow on each date. The BunnyCreekRd_km2 reach appeared to be slightly gaining on three of four dates. The greatest differences occurred for OldmanRd_km14, which exhibited streamflow losses on all measurement dates, with a relative magnitude that increased as flow declined.

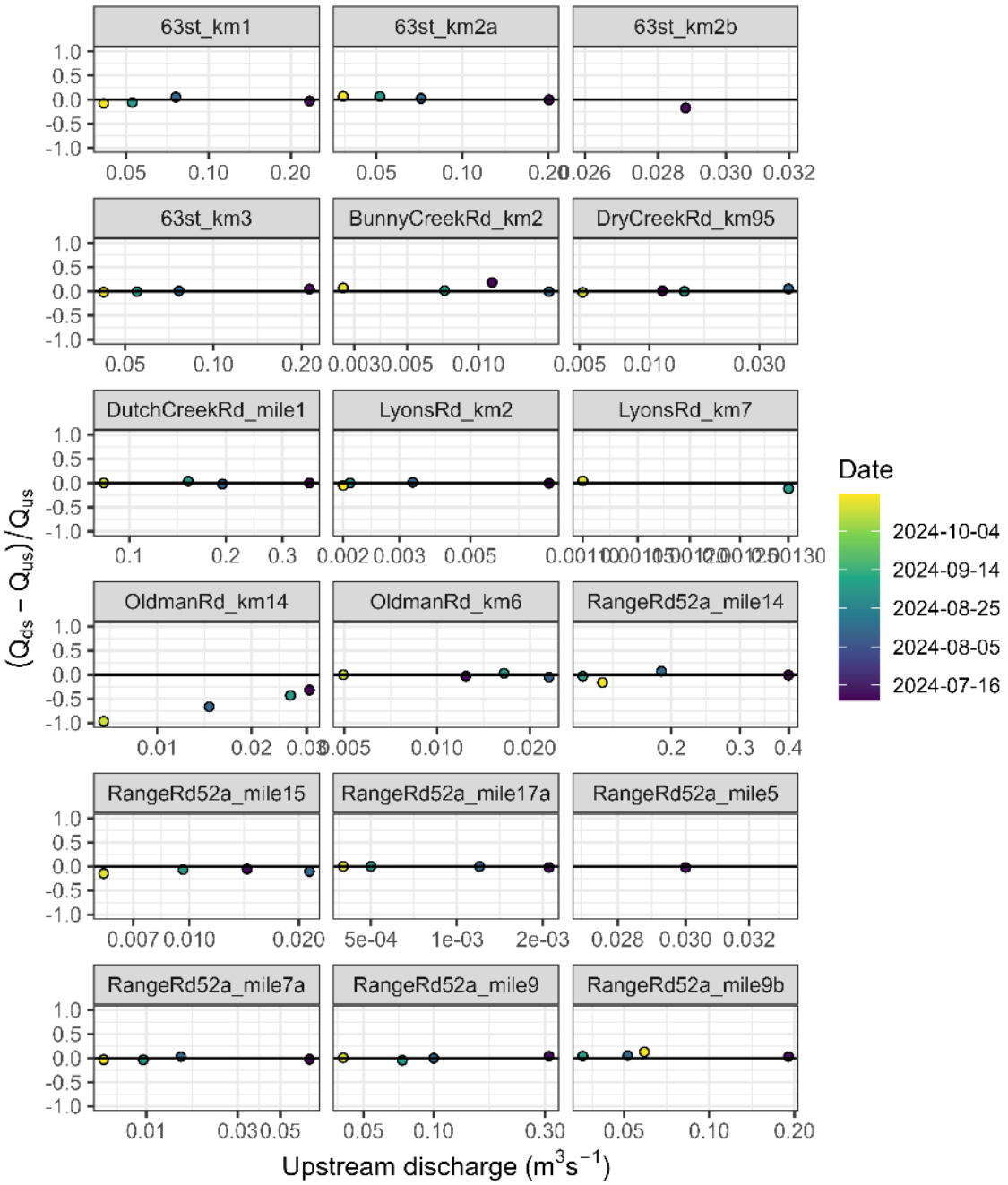

Figure 16 Relative change in streamflow from upstream to downstream as a function of upstream discharge at each site.

Assessment of electrical conductivity focused on observations during July and August, when flows tended to be lowest and stream temperatures highest. While electrical conductivity was relatively constant for most site-dates, some sites displayed variability that could be associated with groundwater discharge (Figure 17). The most marked example is BunnyCreekRd_km2, which displayed a relatively steady increase from logger 1 to logger 5, which is indicative of consistent gaining conditions along the reach and is consistent with the observed downstream increase in streamflow (Figure 16).

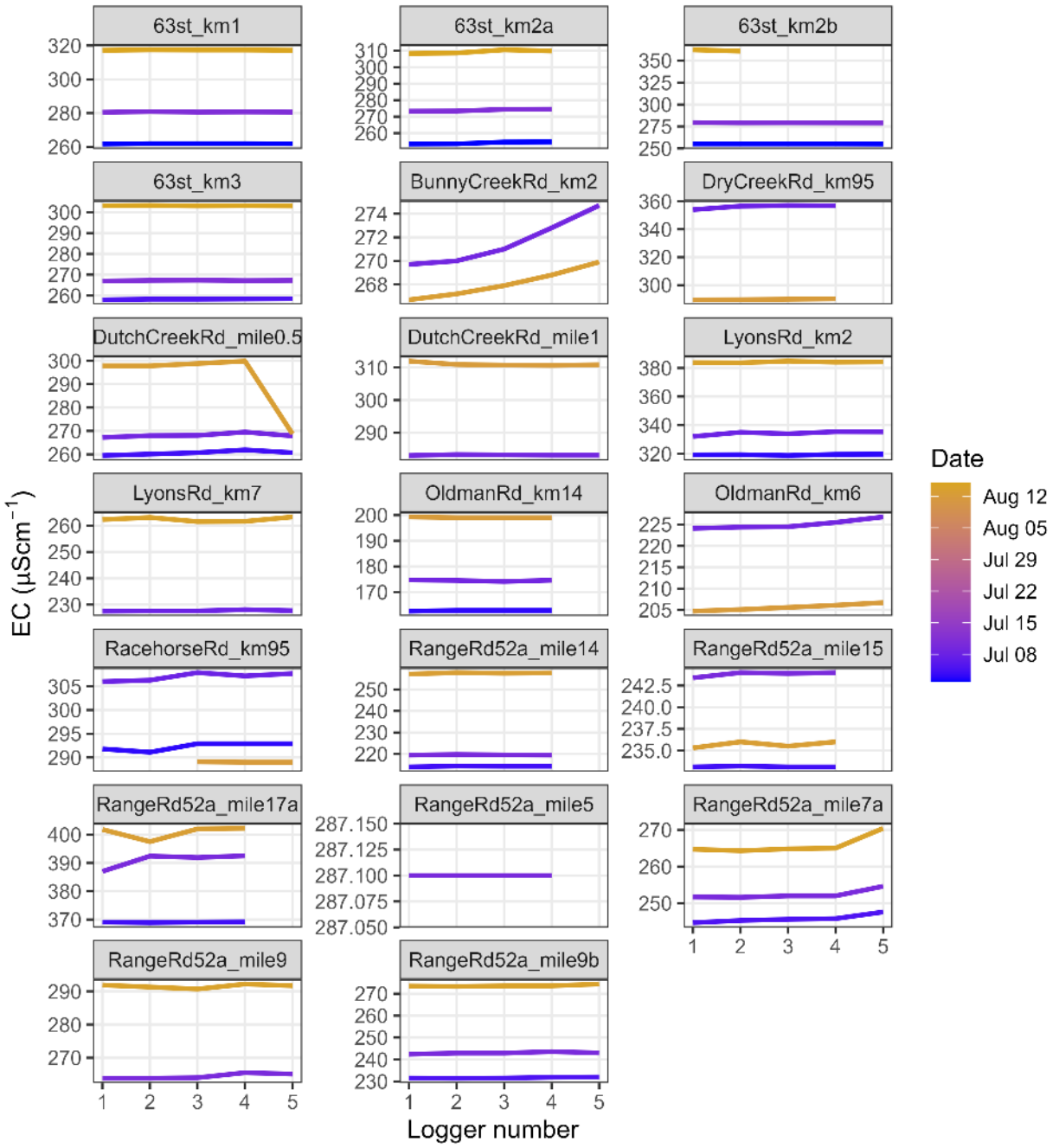

Figure 17 Downstream variations of electrical conductivity during site visits in July and August.

Electrical conductivity at OldmanRd_km6 and DryCreekRd_km95 also displayed relatively consistent but less steep increasing trends during the site visits. Streamflow did increase slightly from upstream to downstream at DryCreekRd_km95, about 1% during the July visit and 5% during the August visit, but these differences are within the typical margin of uncertainty for salt dilution measurements. Streamflow at OldmanRd_km6 decreased by about 5% from upstream to downstream. An increasing trend in EC in the absence of substantial discharge gains or presence of losing conditions could reflect the occurrence of two-way exchanges between the stream and groundwater or the hyporheic zone.

RangeRd52a_mile7a consistently displayed an increase in EC between loggers 4 and 5 during all site visits, suggesting localized groundwater discharge into that segment. However, discharge changed by only about 3% between the upstream and downstream measurements, with a decrease during the July site visit and an increase during the August site visit. It may be that the stream lost flow upstream of logger 4 and then gained a similar amount between loggers 4 and 5.

DutchCreekRd_mile0.5 displayed an abrupt drop in EC in the lowest segment on the last site visit. Like the situation at RangeRd52a_mile7a, this pattern could indicate localized groundwater discharge. However, it could also be a field data entry error.

The change in EC between loggers 1 and 2 at RangeRd52a_mile17a is consistent with discharge of groundwater with EC between about 390 and 400 μS cm^{-1}, resulting in an increase when EC at logger 1 was less than 390 μS cm^{-1} and a decrease when EC at logger 1 was greater than 400 μS cm^{-1}. The increase in EC between loggers 2 and 3 on the last site visit shown (yellow line) suggests the occurrence of groundwater discharge with EC greater than the recorded EC at logger 2 on that date.

5.7 Temporal variability of stream temperature

Figure 18 reveals a range of thermal patterns for a three-day period during which most sites experienced their highest temperatures and the maximum downstream temperature changes in the right-of-way segments. DutchCreekRd_mile1, DutchCreekRd_mile0p5, 63st_km3, RangeRd52a_mile5 and RangeRd52a_mile9b exhibited relatively minor changes in the magnitude or timing of the diel cycle. Some displayed a downstream increase in and earlier timing of the daily maximum, such as 63St_km1, RangeRd52a_mile17 and BunnyCreekRd_km2. In contrast, OldmanRd_km14 and LyonsRd_km7 exhibited a later maximum. Some sites showed downstream changes for the whole diel cycle, such as LyonsRd_km7 and RangeRd52a_mile7a, whereas others differed mainly around the daily peak, such as 63st_km1 and DryCreekRd_km95. Longer-term temporal variability within and among each of the sites are shown in time series plots in Appendix A.

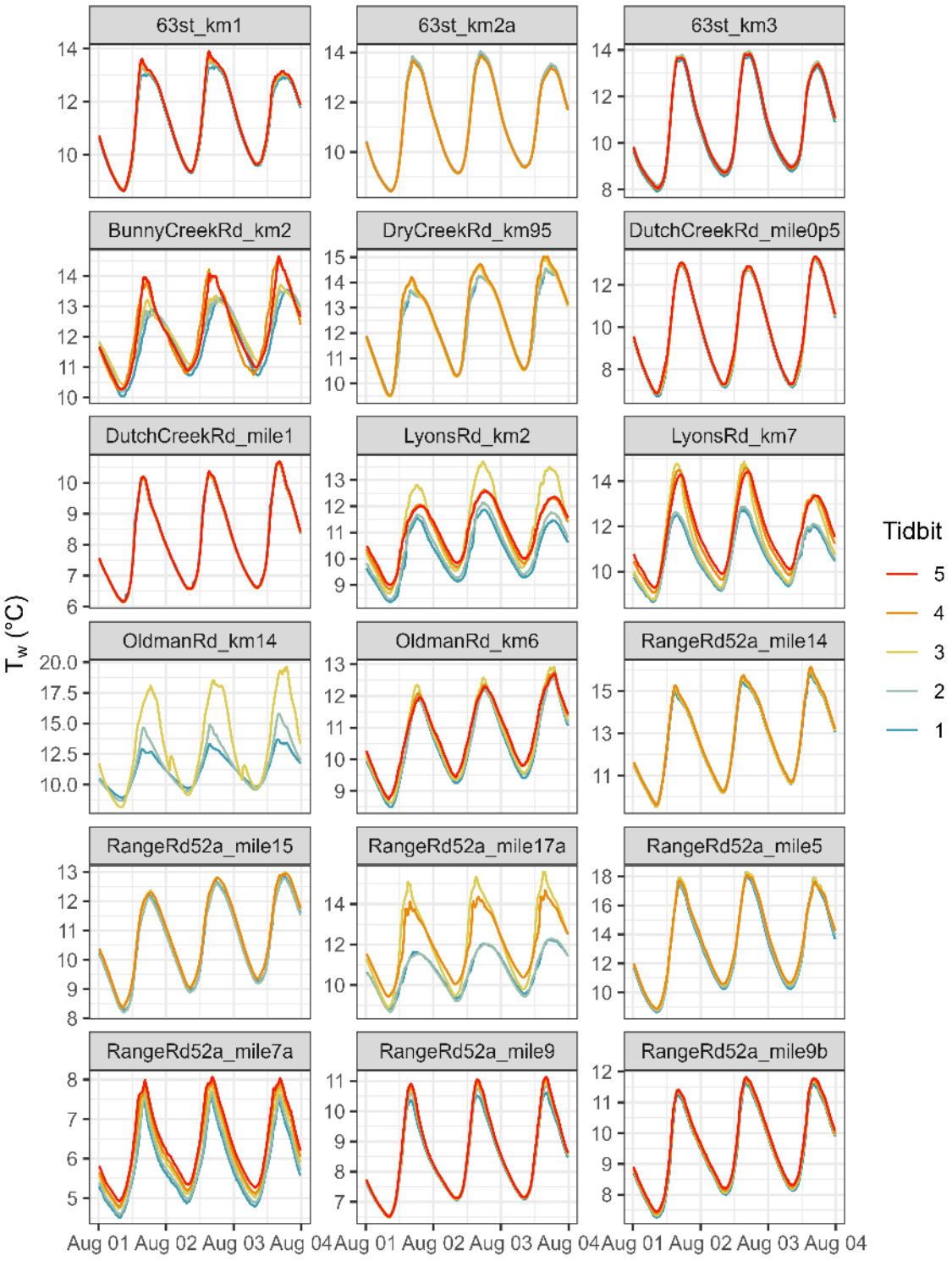

Figure 18 Diel stream temperature variations at all sites and loggers for August 1 to 3, when most sites reached their maximum temperatures during the study period. Site 1 to 5 are upstream to downstream, respectively, with sites 1 and 2 above the road crossing.

5.8 Downstream temperature changes within each segment

Figures 19, 20 and 21 illustrate time series of the downstream changes in daily maximum, mean and minimum stream temperatures for each segment at each site. For most sites, downstream temperature changes were generally within the nominal uncertainty of $\pm$ 0.4 °C. The main exceptions are for LyonsRd_km2, LyonsRd_km7, OldmanRd_km14 and RangeRd52a_mile17a, for which the maximum and mean temperatures tended to increase through the segment while the minimum temperatures tended to decrease, especially toward the end of the study period.

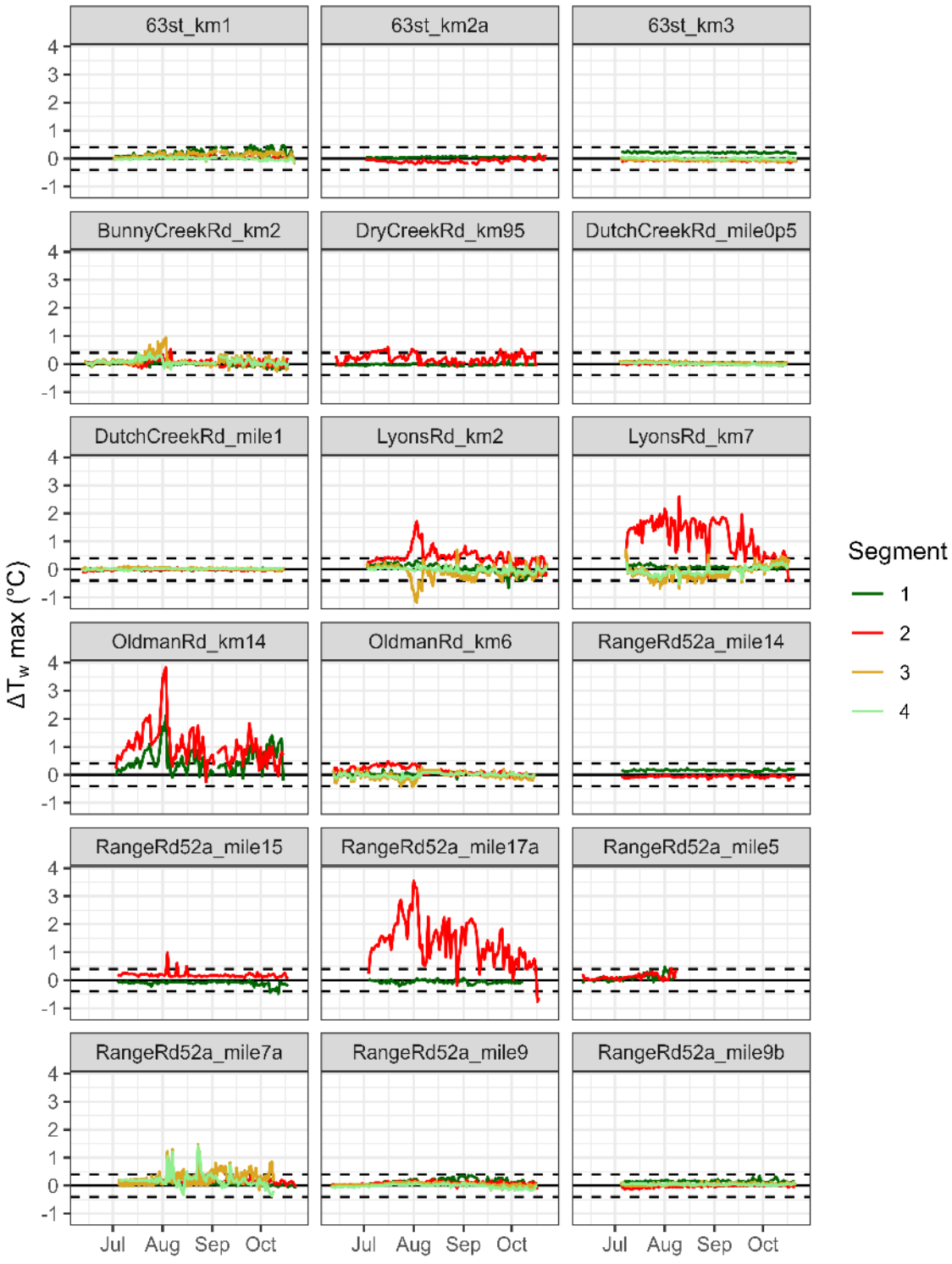

Figure 19 Time series of the change in daily maximum stream temperature between the upstream and downstream ends of each segment. The dashed horizontal lines indicate an approximate uncertainty in the downstream temperature change of ± 0.4 °C.

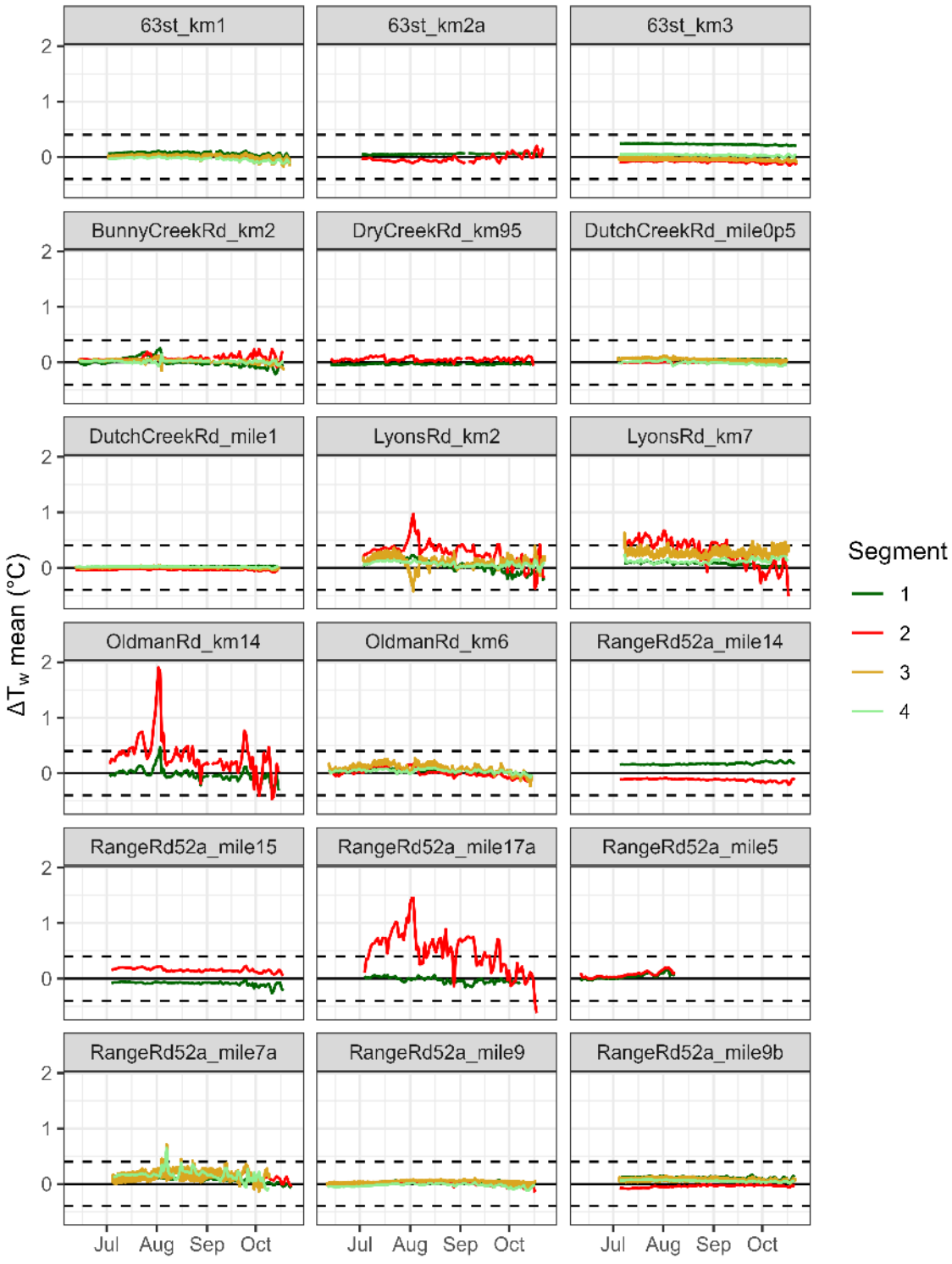

Figure 20 Time series of the change in daily mean stream temperature between the upstream and downstream ends of each segment. The dashed horizontal lines indicate an approximate uncertainty in the downstream temperature change of ± 0.4 °C.

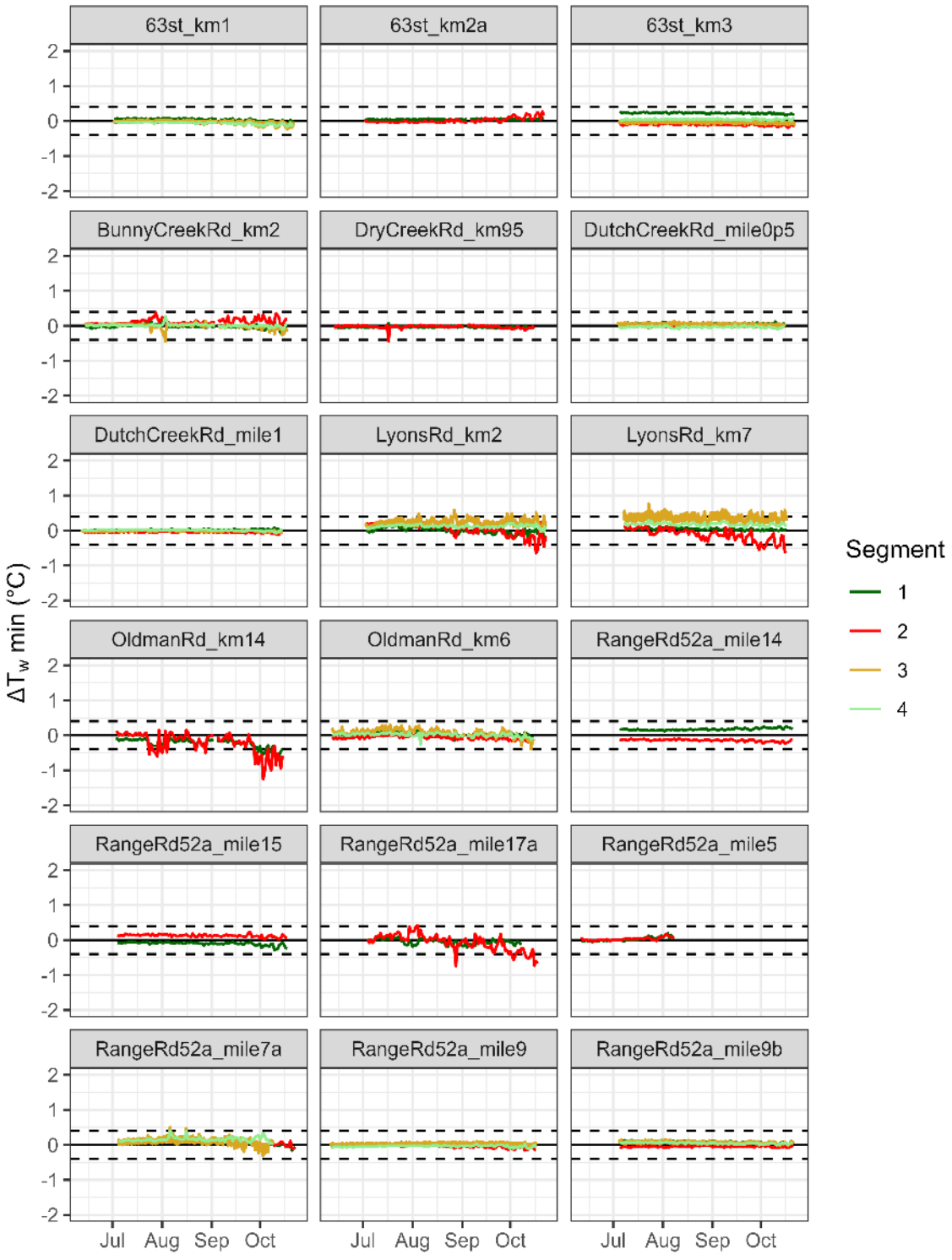

Figure 21 Time series of the change in daily minimum stream temperature between the upstream and downstream ends of each segment. The dashed horizontal lines indicate an approximate uncertainty in the downstream temperature change of ± 0.4 °C.

Figure 22 compares changes in the daily maximum stream temperatures through the road right-of-way compared to the upstream reference segment. Temperature changes through the reference segment were mostly within the nominal uncertainty of ± 0.4 °C at all but two sites. One exception was the LyonsRd_km2 site, where daily maximum temperatures frequently decreased through the reference segment by up to almost 1 °C. The other was the OldmanRd_km14 site, where daily maximum stream temperature increased by up to slightly more than 2 °C.

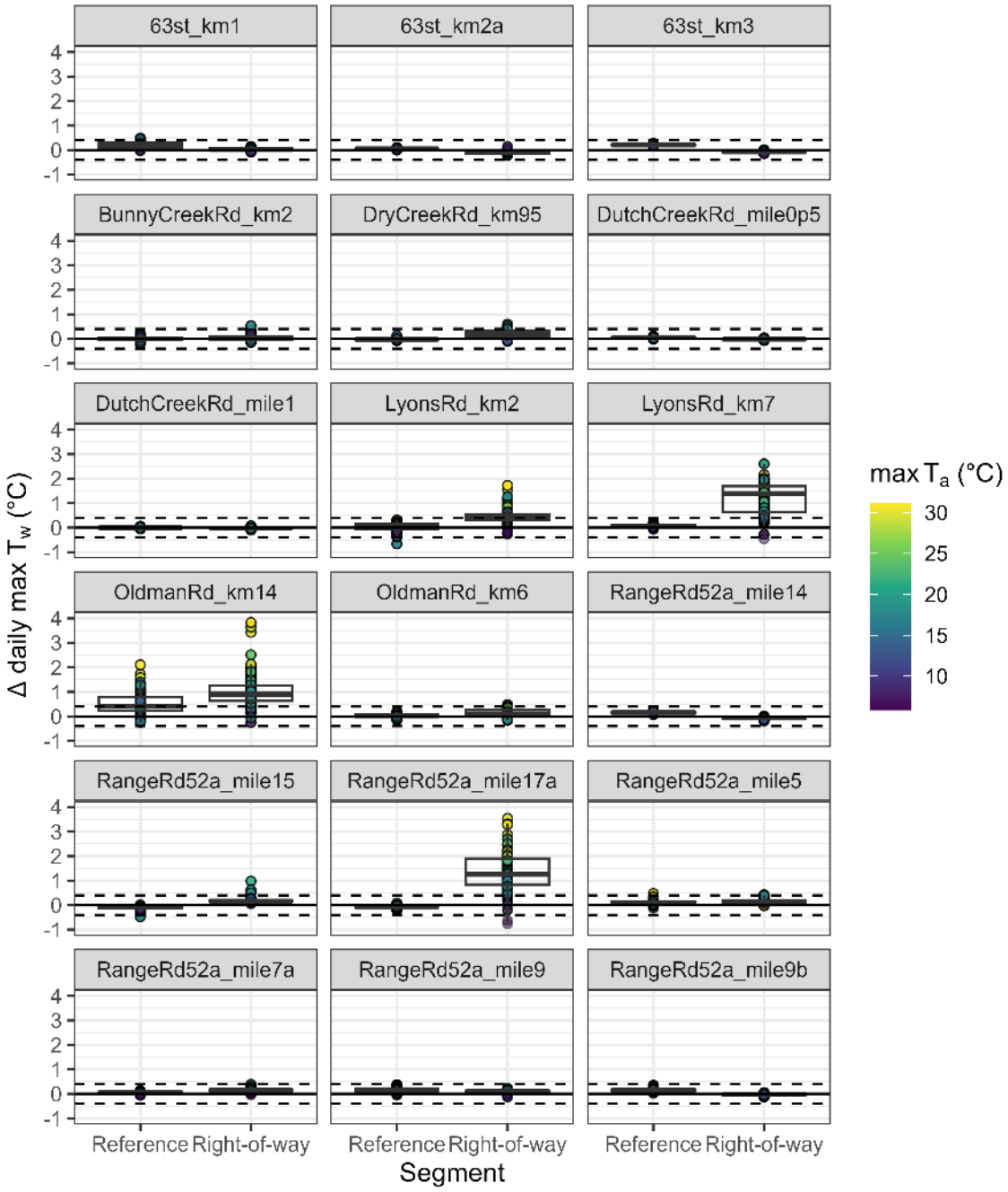

Figure 22 Boxplots comparing the difference in daily maximum Tw between loggers 3 and 2 (the right-of-way) and loggers 2 and 1 (the reference segment). Symbol colour indicates daily maximum air temperature.

The dashed horizontal lines indicate an approximate uncertainty in the downstream temperature change of ± 0.4 °C.

Changes in daily maximum stream temperature through the right-of-way segment were notably different from those in the reference segment at four sites, with the greatest increase of about 4 °C at the OldmanRd_km14 site. The magnitude of temperature change through the right-of-way segments, and through the reference segment for OldmanRd_km14, appeared to be positively correlated with the daily maximum air temperature, with the largest increases associated with high daily maximum air temperatures.

Changes in daily mean temperature through the reference and right-of-way segments displayed similar patterns to those for daily maximum temperature, but with lower magnitudes (Figure 23). For example, the maximum increase at the OldmanRd_km14 site was about 2 °C, about half that for the daily maximum stream temperature.

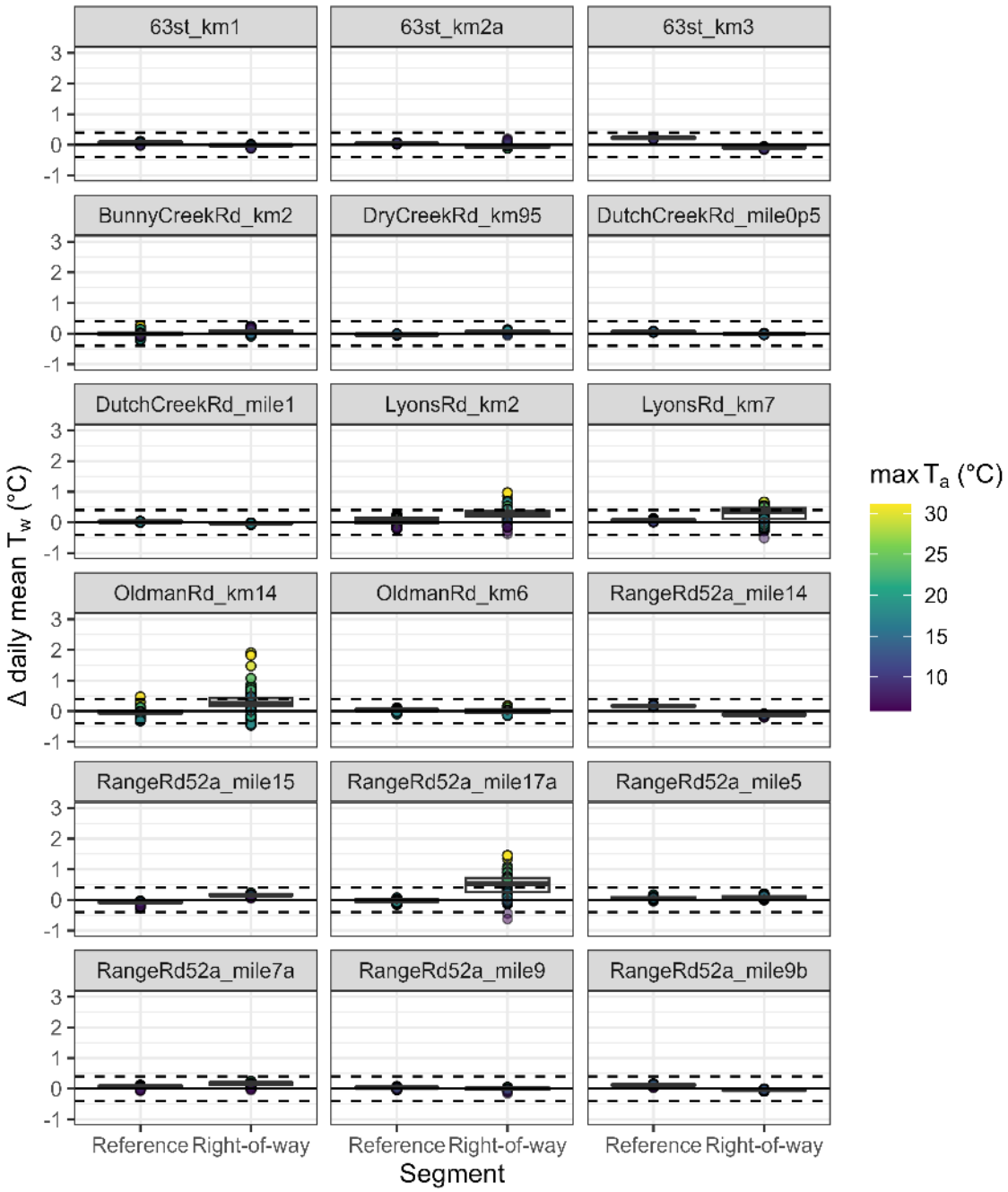

Figure 23 Boxplots comparing the difference in daily mean Tw between loggers 3 and 2 (the right-of-way) and loggers 2 and 1 (the reference segment). Symbol colour indicates daily maximum air temperature. The dashed horizontal lines indicate an approximate uncertainty in the downstream temperature change of ± 0.4 °C.

Changes in daily minimum stream temperature exhibited relatively minor changes at all sites for both reference and right-of-way segments, dominantly within ± 0.4 °C (Figure 24). However, the sites that exhibited the greatest changes in daily maximum temperature through the right-of-way segment – LyonsRd_km2, LyonsRd_km7, OldmanRd_km14, and RangeRd_mile17a – tended to exhibit downstream decreases in daily minimum temperature.

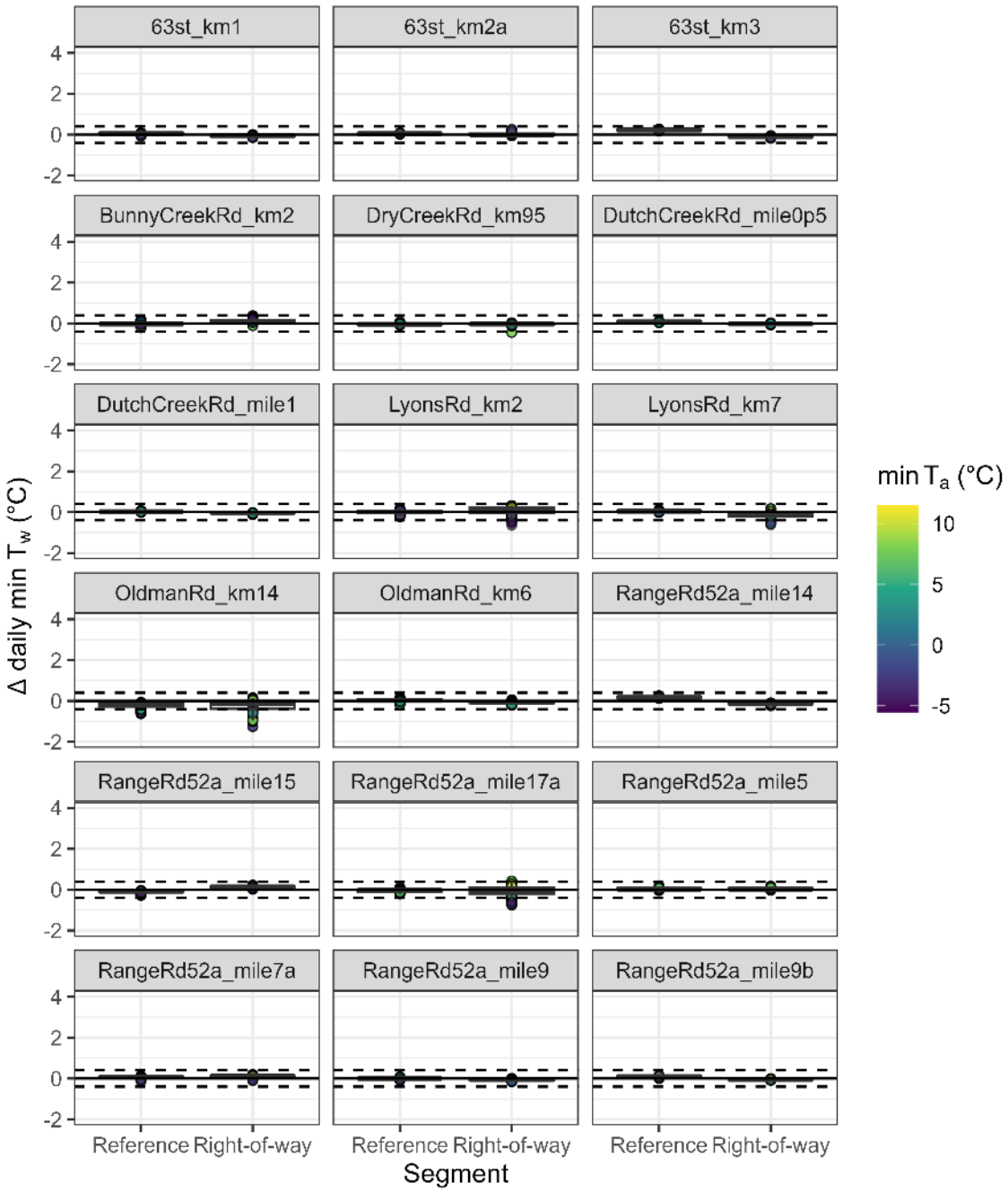

Figure 24 Boxplots comparing the difference in daily minimum Tw between loggers 3 and 2 (the right-of-way) and loggers 2 and 1 (the reference segment). Symbol colour indicates daily minimum air temperature. The dashed horizontal lines indicate an approximate uncertainty in the downstream temperature change of ± 0.4 °C.

5.9 Temporal variability of temperature changes in the right-of-way segment

As seen in Figure 25, the magnitude of warming in the right-of-way segment generally increased through July and into early August. During this period, daily maximum air temperature was relatively stable at around 30 °C with the exception of a series of cooler days in the latter part of July, and solar radiation was also relatively stable, while streamflow steadily declined with the exception of a transient response to a rain event in mid-July. After the first week of August, air temperatures and solar radiation were lower than during July while streamflow remained relatively constant. Warming through the right-of-way segment during this period generally responded to day-to-day changes in air temperature, but remained lower than during the first week of August.

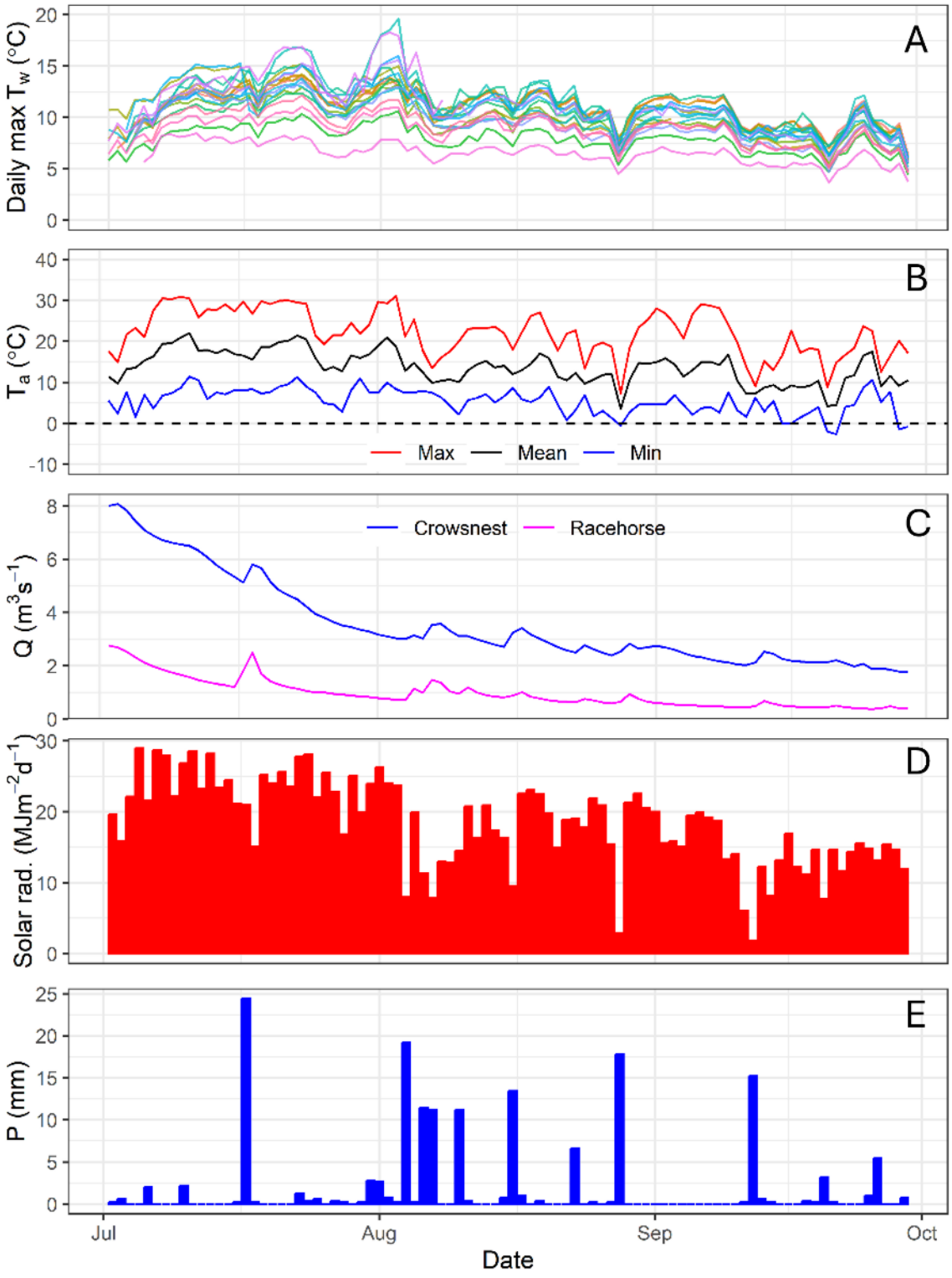

Figure 25 Hydrometeorological conditions during the study period. From top to bottom, the panes show (a) time series of daily maximum temperature at logger 3 for each site (distinguished by colour); (b) daily maximum, mean and minimum air temperature at the South Racehorse Creek weather station; (c) daily mean streamflow at the Crowsnest River and Racehorse Creek gauging stations; (d) daily global solar

radiation at the South Racehorse Creek weather station; and (e) daily total rainfall at the South Racehorse Creek weather station.

Figure 26 illustrates the dependence of changes in daily maximum temperature through the right-of-way segment on daily maximum air temperature and scaled discharge. The latter was computed by dividing each predicted daily discharge by the maximum at the site. There is a positive association between $\Delta maxT_w$ and daily maximum air temperature at LyonsRd_km2, LyonsRd_km7, OldmanRd_km14 and RangeRd52a_mile17a – i.e., all the sites that had experienced downstream warming greater than 1 °C. In addition to the association with daily maximum air temperature, there is an apparent dependence on discharge, particularly on days with high air temperature, as indicated by the darker blue points plotting below the lighter-coloured points for a given air temperature.

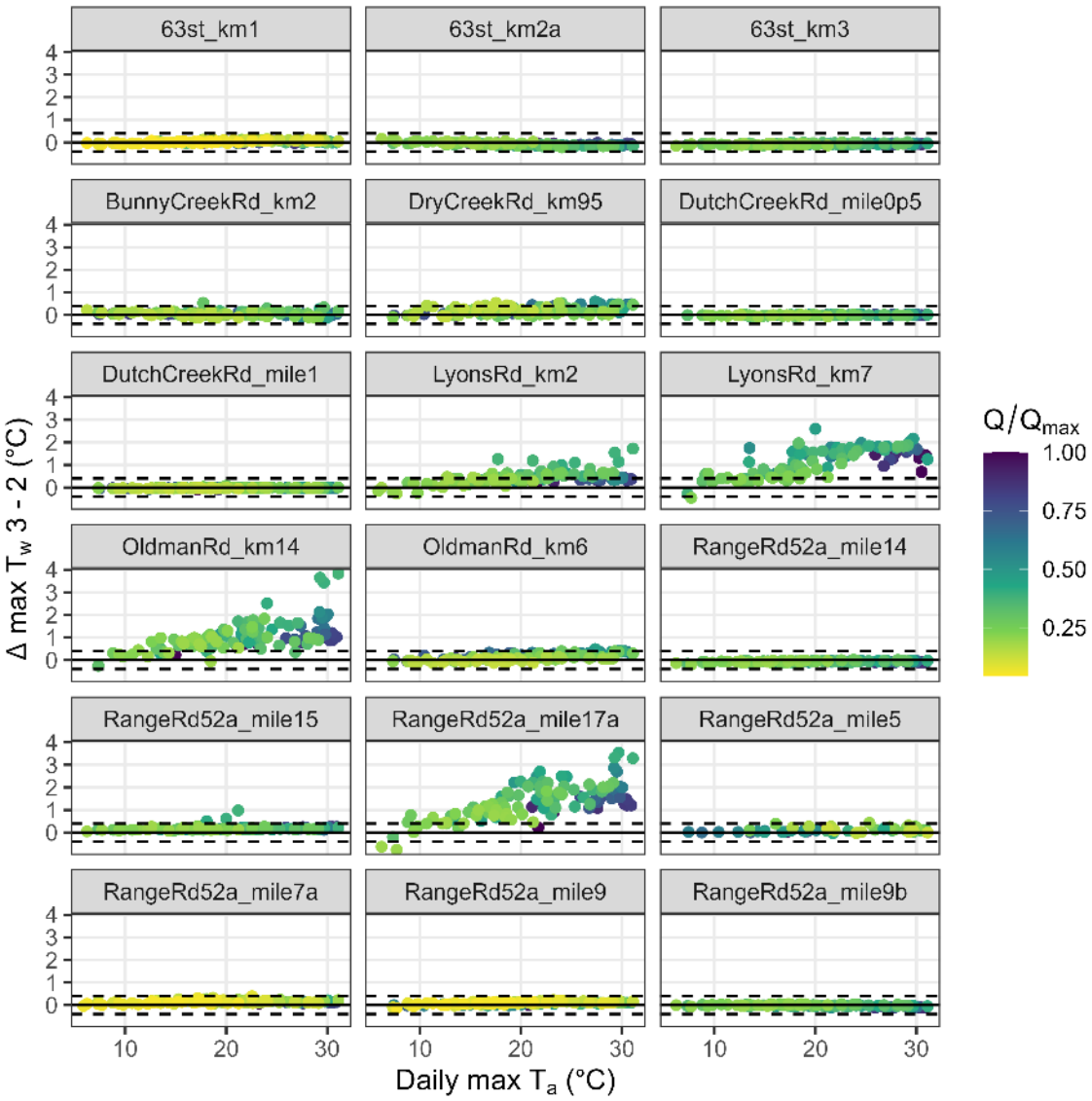

Figure 26 Changes in daily maximum temperature through the right-of-way segment (between sites 2 and 3) in relation to daily maximum air temperature and discharge estimates at each site. Discharge values have been scaled by dividing by the maximum value for the study period to highlight temporal variability at each site rather than variability across sites.

5.10 Downstream temperature changes through the reference and right-of-way segments in relation to site factors

Figure 27 and Figure 28 illustrate the associations between downstream temperature changes through the right-of-way and site characteristics. While the sample size is too small to draw firm conclusions, it does appear that increases greater than 0.4 °C are restricted to sites with upstream catchment areas

less than 10 km^2. In terms of bankfull width, a threshold for increases greater than 0.4 °C appears to lie between 3 and 5 m.

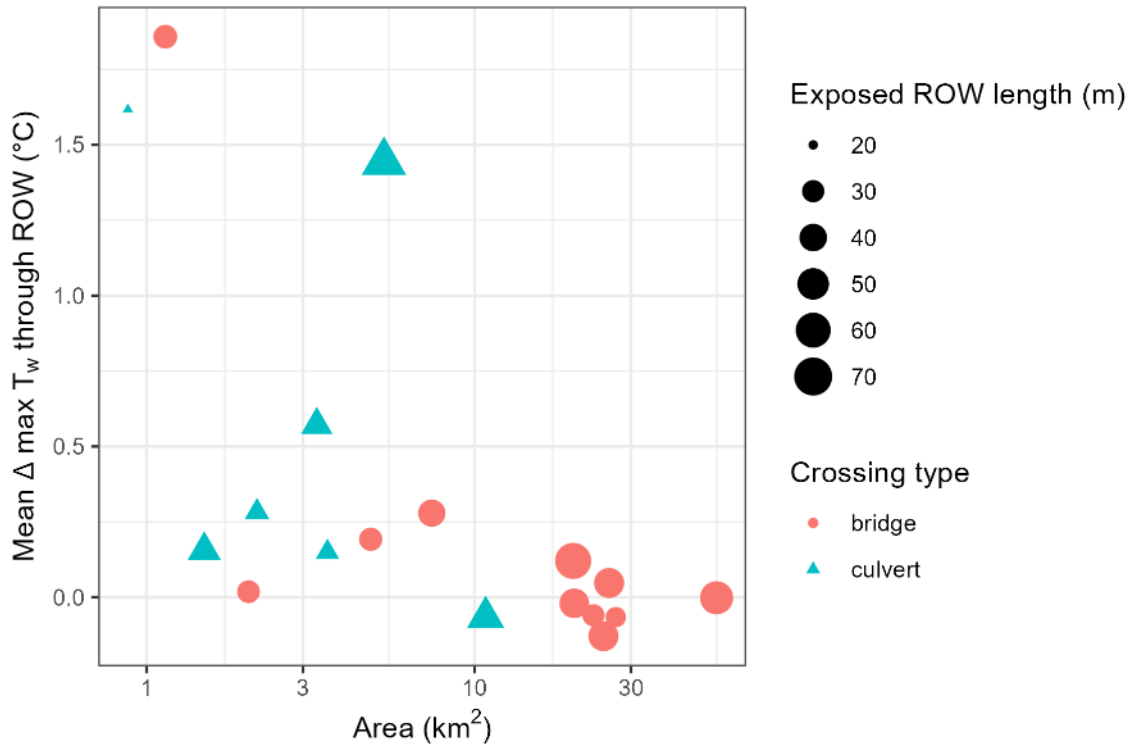

Figure 27 Mean value of change in daily maximum temperature through the right-of-way segment for days with maximum air temperature greater than 25 °C, in relation to upstream catchment area, crossing type and exposed length of stream in the right-of-way.

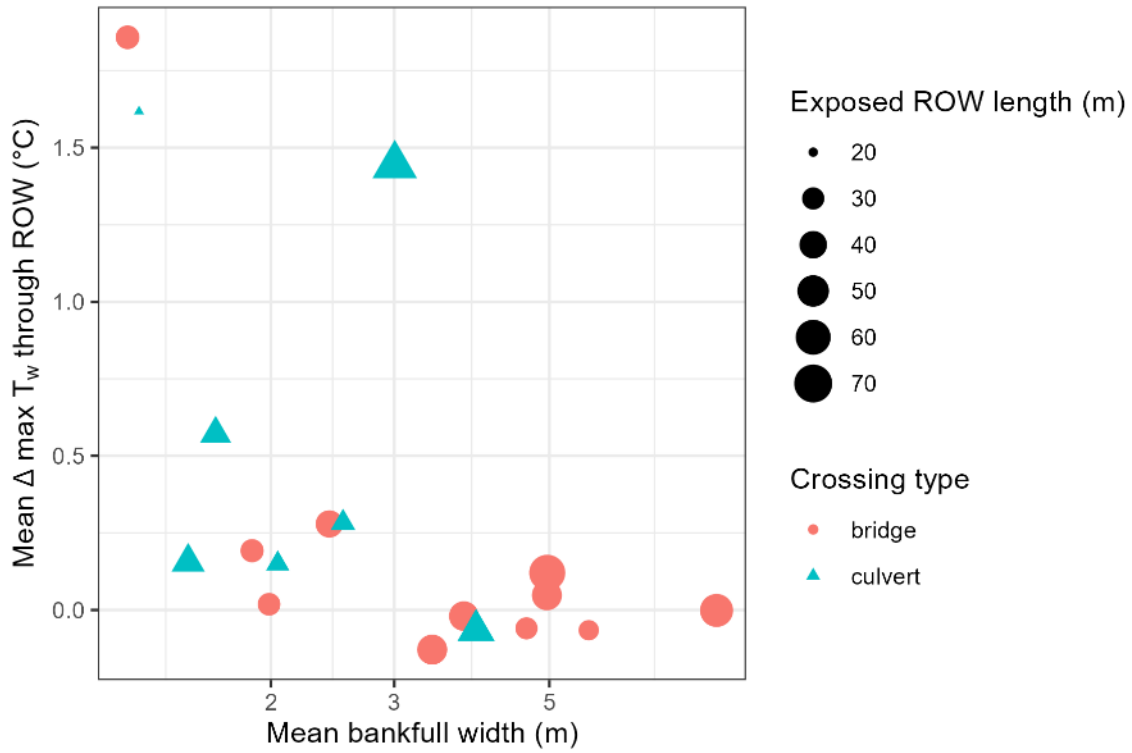

Figure 28 Mean value of change in daily maximum temperature through the right-of-way segment for days with maximum air temperature greater than 25 °C, in relation to upstream catchment area, crossing type and exposed length of stream in the right-of-way.

Figure 29 illustrates the relationship for a sample of days between the downstream change in daily maximum T_w and the integrated measure of above-stream solar radiation. For sites with upstream catchment areas greater than 10 km^2, temperature changes remained within $\pm$ 0.4 °C regardless of energy input or daily maximum air temperature. For sites with catchment areas less than 10 km^2, there appeared to be date-specific thresholds of the integrated solar radiation input, below which the downstream temperature change remained within $\pm$ 0.4 °C regardless of energy input or daily maximum air temperature. Above the threshold, some sites exhibited strong temperature changes, up to almost 4 °C, while others exhibited little change.

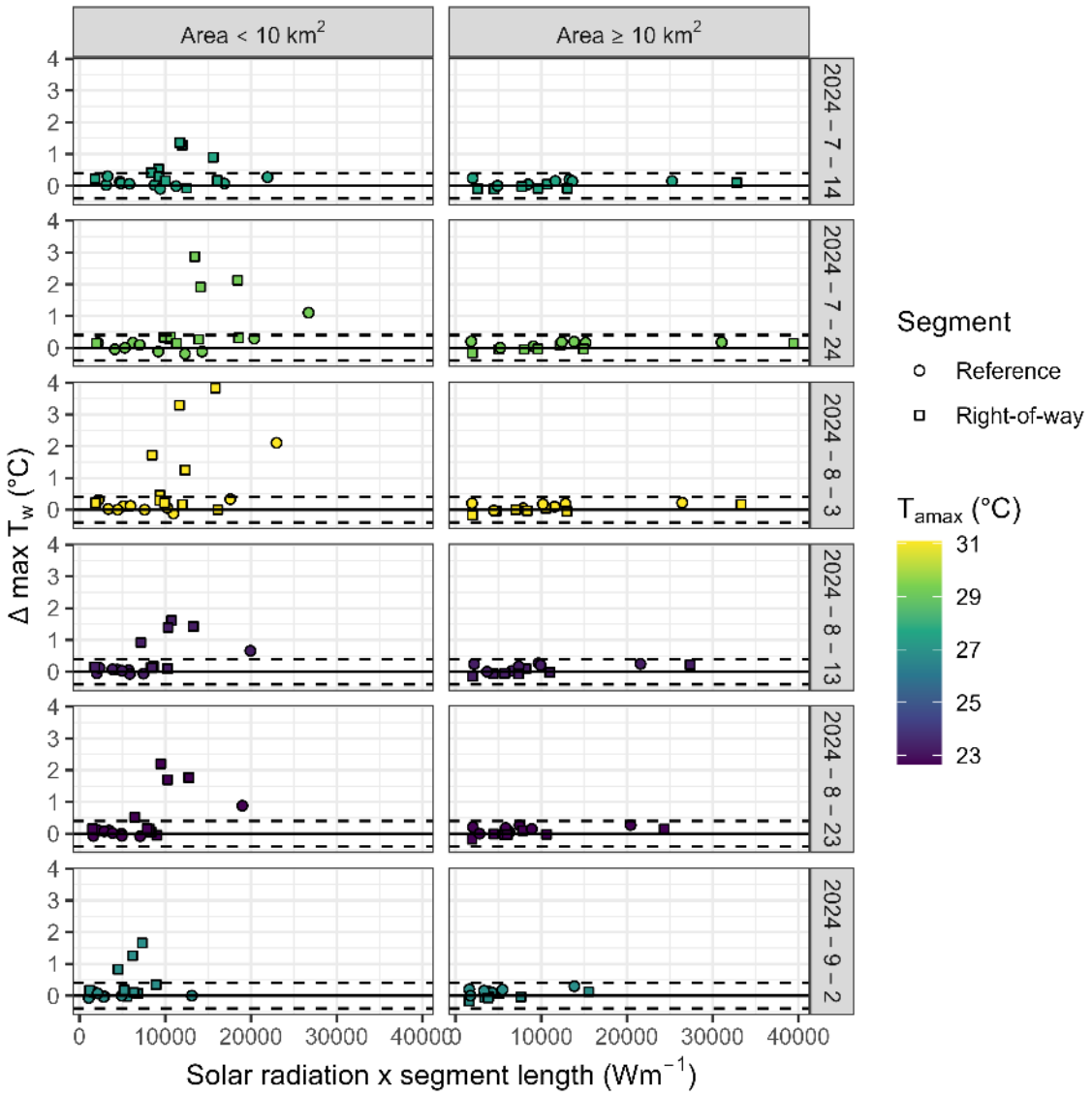

Figure 29 Change in daily maximum temperature through the reference and right-of-way segments sampled at a 10-day interval from mid-July to early September, including the day on which the maximum change occurred (August 3, 2024). in relation to upstream catchment area, crossing type and exposed length of stream in the right-of-way.

5.11 Downstream persistence of right-of-way warming

Temperature changes in the segment immediately downstream of the right-of-way varied among sites in both magnitude and direction (Figure 30). Sites with warming of less than about 0.4 °C within the right-of-way exhibited either a similarly small change in the segment between loggers 3 and 4 (e.g., 63st_km1 and RangeRd52a_mile9b) or warming up to about 1 °C (e.g., BunnyCreekRd_km2). Six sites had increases in daily maximum temperature of up to 1 °C or greater through the right-of-way segment. Of these sites, LyonsRd_km2 exhibited close to a 1:1 cooling in the segment between loggers 3 and 4. RangeRd52a_mile9 had minimal decrease except when the increase in the right-of-way exceeded about 2 °C, while the LyonsRd_km7 and RangeRd52a_mile15 exhibited minimal change. Two sites,

BunnyCreekRd_km2 and OldmanRd_km14, exhibited increases in daily maximum temperature in the segment between loggers 3 and 4.

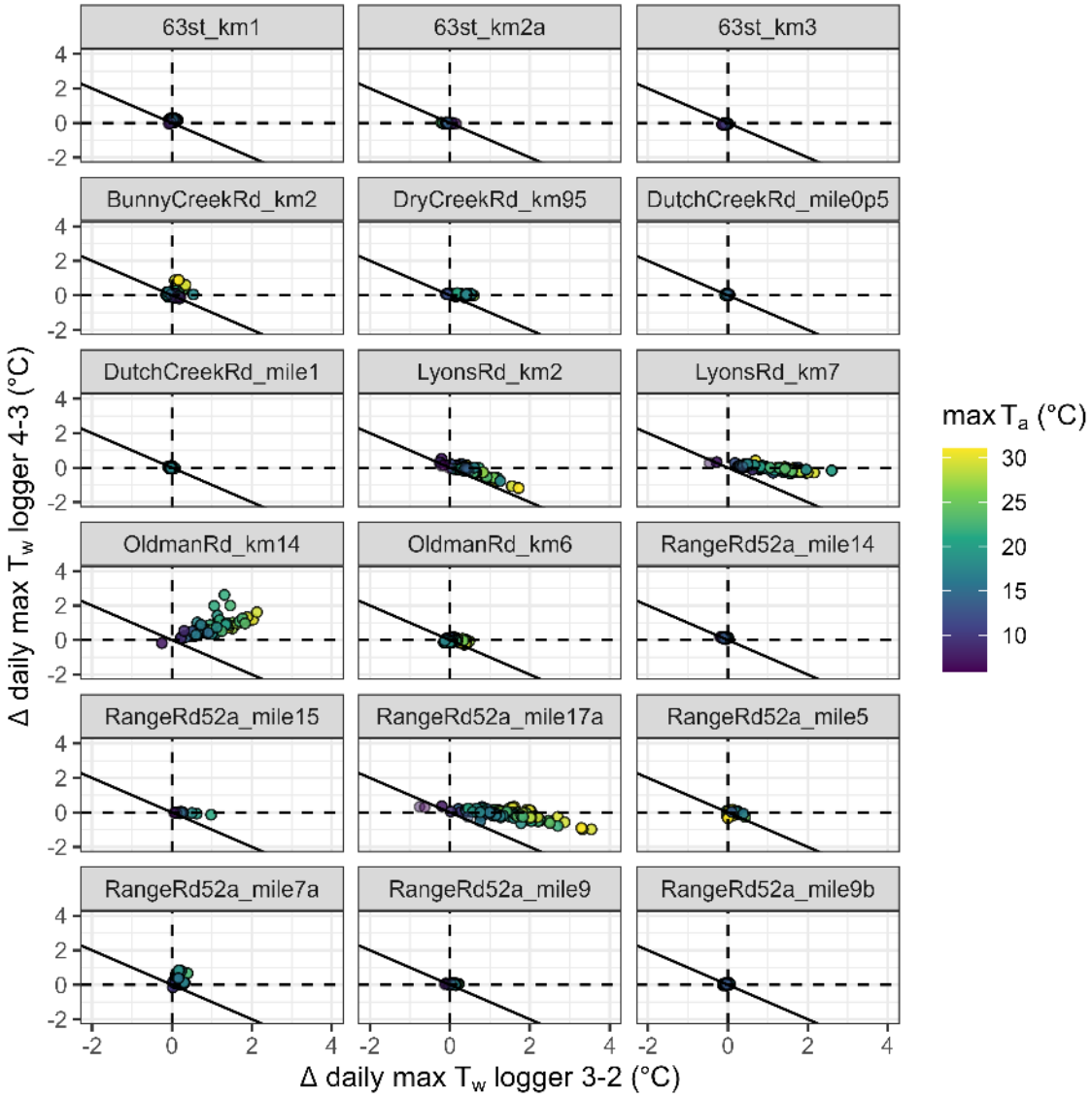

Figure 30 Plot of changes in daily maximum Tw for the segment between loggers 3 and 4 versus changes through the right-of-way. The solid line with a slope of -1 provides a visual reference representing downstream cooling equal to warming in the right-of-way segment. Points above zero indicate warming and below zero indicate cooling.

Figure 31 shows downstream temperature changes between loggers 3 and 5 for stations with 5 loggers. BunnyCreekRd_km2 and RangeRd52a_mile7a, both of which had temperature increases through the right-of-way of about 0.4 °C or less, exhibited increases in daily maximum temperature downstream of the right-of-way. The two sites with increases of greater than 0.4 °C through the right-of-way, LyonsRd_km2 and to a lesser extent LyonsRd_km7, exhibited downstream decreases in daily maximum temperature, at least for the days with the greatest increases in the right-of-way segment.

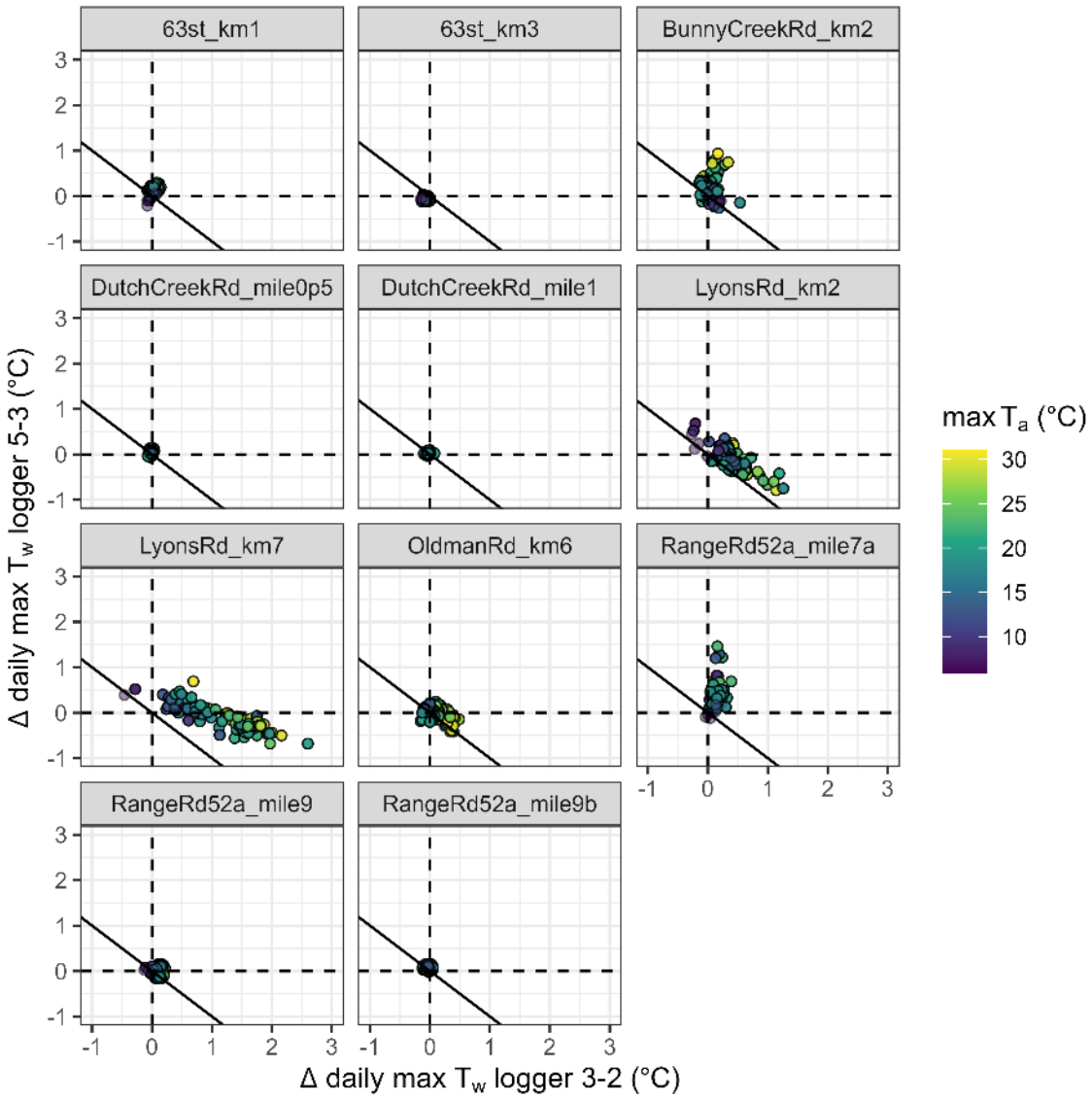

Figure 31 Plot of changes in daily maximum Tw for the segment between loggers 3 and 5 versus changes through the right-of-way. The solid line with a slope of -1 provides a visual reference representing downstream cooling equal to warming in the right-of-way segment. Points above zero indicate warming and points below zero indicate cooling.

6 Discussion

6.1 Temperature changes in the reference segments

As seen in Figure 22, downstream warming in the reference reaches was generally less than 0.4 °C at all sites except OldmanRd_km14. That site differed from the others in that it had experienced a debris flow, likely in 2013, and the regenerating forest had not developed to the point of providing shade equivalent to an undisturbed, mature riparian forest stand. The relative lack of shading is illustrated in Figure 14. In a similar vein, Dunham *et al.* (2007) found that streams that experienced substantial channel reorganization following wildfires were more likely to experience high (> 20 °C) water temperatures than unimpacted streams or fire-disturbed streams without channel reorganization.

If the stated accuracy of the TidbiT loggers, 0.2 °C, is taken to be a two-sigma uncertainty, then the difference between temperatures measured by two loggers should have a two-sigma uncertainty of about 0.3 °C and a worst-case uncertainty of 0.4 °C. Therefore, it appears that much of the apparent warming at all sites except OldmanRd_km14 is within the margin of uncertainty. An important implication is that, for sites with undisturbed forest, the maximum natural warming over the segment lengths used in this study is likely to be, at most, 0.4 °C. Therefore, the difference in temperature between loggers 2 and 3 is likely to be a slight over-estimate of the effect of the road and right-of-way clearing.

One caveat to this statement is that a segment with low flow and high rates of groundwater discharge could exhibit downstream cooling in the absence of disturbance, in which case the temperature change between loggers 2 and 3 would be an underestimate of warming associated with the road and right-of-way. However, such a site would likely exhibit an increase in discharge between the upper and lower ends of the reach, and/or a marked increase in electrical conductivity between loggers 2 and 3 that would be sustained to the lower boundary of the reach. Based on examination of Figures 16 and 17, the BunnyCreekRd_km2 site appears to be the most likely to have been influenced by groundwater discharge in the right-of-way segment.

6.2 Temperature changes in the right-of-way segments

Temperature changes through the right-of-way segments were greatest for daily maxima and smallest for daily minima. This pattern is consistent with results reported for various forest harvesting treatments (Gomi *et al.*, 2006; Guenther *et al.*, 2014; Oanh *et al.*, 2021) and reflects the fact that daytime solar radiation is the main driver of stream warming following riparian forest disturbance.

Four sites exhibited downstream warming in the right-of-way segments outside the bounds of both sensor uncertainty and background rates of downstream warming: LyonsRd_km2, LyonsRd_km7, OldmanRd_km14 and RangeRd52a_mile17a. These sites had upstream catchment areas less than 10 km^2, but had a mix of crossing types (three have culverts) and a range of exposed stream lengths in the right-of-way, from 20 to 60 m. This dependence of the magnitude of warming on upstream catchment area is consistent with physical principles and with empirical studies such as Coats and Jackson (2020). Larger catchments are associated with higher streamflow which, in turn, is associated with increased stream depth and velocity, both of which tend to reduce warming as water flows downstream.

The maximum warming in the right-of-way segments occurred during the first week of August. As seen in Figures 6 and 7., this period had high air temperatures and low streamflow relative to the longer-term

historical record, conditions that are conducive to stream warming (e.g., Oanh *et al.*, 2021; Moore *et al.*, 2023).

The four right-of-way segments that exhibited marked increases in daily maximum stream temperature tended to exhibit downstream decreases in daily minimum stream temperature, particularly toward the end of the study period. This cooling likely reflects the effect of increased losses of longwave radiation on cool nights due to reduced emission from the surrounding forest canopy in the right-of-way segments. Coats and Jackson (2020) showed similar findings, demonstrating smaller streams can warm more in openings and cool more rapidly in shaded areas.

While it is not possible to draw a firm conclusion from the sample, it appears that the risk of thermal impacts should be greatest for smaller catchments, specifically those with catchment areas less than 10 km^2. However, as seen in Figures 27 and 28, those smaller catchments exhibited a range of temperature changes. This range in responses likely relates to the effects of variations in channel morphology and hydrology (as well as surface-sub surface interactions) among sites, as illustrated and discussed by Gomi *et al.* (2006) and Janisch *et al.* (2012) and explored in the following section.

6.3 Distinctive effects of reach-scale hydrology

Distinctive effects of reach-scale hydrology can be inferred from the diel temperature patterns as presented in Section 4.7. For example, sites at which both maxima and minima increased through the right-of-way segment (e.g., see LyonsRd_km2 and LyonsRd_km7 in Figure 18) are likely influenced by higher rates of hyporheic exchange, which would result in heat from daytime solar exposure being stored in the stream bed and released at night. These sites could be particularly sensitive to hyporheic exchange given that they had the lowest measured discharges among the sample (see Figure 11).

Increases in daytime maxima and decreases in late-morning minima, as seen at OldmanRd_km14, suggest a lesser degree of dynamic heat exchange with the bed. As mentioned above, the OldmanRd_km14 site was influenced by a debris flow that caused aggradation, which, in turn, is conducive to streamflow losses by infiltration into the streambed. Such losses are evidenced by the consistent downstream flow losses shown in Figure 16. Downward advective heat transport in the bed would tend to reduce upward heat conduction at night, thus making the stream more sensitive to nocturnal heat loss.

6.4 Downstream persistence of warming in the right-of-way segments

Of the four sites that exhibited significant warming through the right-of-way segment, one (LyonsRd_km2) also exhibited close to a 1:1 cooling in the segment between loggers 3 and 4. As mentioned in Section 5.2, downstream changes in the diel cycle suggest that this site may be influenced by hyporheic heat storage, which can drive downstream cooling in shaded environments (e.g. Story *et al.*, 2003).

The LyonsRd_km7 site did not exhibit any downstream cooling in the segment between loggers 3 and 4, but did exhibit minor cooling of up to about 0.5 °C when considering the segment between loggers 3 and 5. The OldmanRd_km14 site exhibited continued warming in the segment between loggers 3 and 4, likely due to the relative lack of shade due to disturbance by the debris flow.

The BunnyCreekRd_km2 site exhibited relatively minor warming in the right-of-way segment, less than 1 °C, with warming of up to about 1 °C in the segment between loggers 3 and 4, which persisted down

to logger 5. An unusual aspect of this site is the fact that the stream flows roughly west to east in an incised valley and the road roughly follows the contour in its approach to the stream from the south. Consequently, the road and its right-of-way result in reduced shading in the segment between loggers 3 and 4.

6.5 Implications for fish and fish habitat

This study suggests thermal regimes of small streams (< 3 m with and < 10 km^2 watershed area) are more sensitive to stream crossings (Figure 27 and Figure 28). No fish were observed during this study; however, the streams sampled here are within the range of habitats identified as critical for westslope cutthroat trout and bull trout. These small streams could support important life stages by providing:

- Spawning and rearing habitats
- Thermal refugia during hot (or cold) periods
- Food sources from benthic invertebrates

Field sampling suggests that stream temperature preference for westslope cutthroat trout is < 16 °C (Behnke and Zarn 1976; McIntryre and Rieman 1995) but laboratory studies from Alberta populations suggest that preferences may be higher between 17.7-20.6 °C (Macnaughton et al. 2018) with performance peaking around 15 °C (Macnaughton et al. 2021). When considering bull trout optimal temperature, the field and laboratory would suggest they occur and function better at cooler temperatures (~ 10 - 15 °C, Selong et al. 2001; Dunham et al. 2003). All streams within our study were at or below the thermal range for westslope cutthroat trout and bull trout. Despite this, observations of daytime maximum stream temperatures nearing 20 °C at multiple sites would suggest that some of these sites might not be ideal for westslope cutthroat trout or bull trout during peak temperatures and would result in daily or seasonal movements to cooler waters (Isaak and Young 2023). Knowing that most of these streams had no measurable change in water temperature through the road right of way is encouraging as many watersheds in Alberta are at the thermal edge for native trout species and subtle changes from various sources could restrict available habitat greatly (Isaak et al. 2012). Though many of the sites had little change, observed increase up to ~4 °C through the right of way pose significant challenges for fish especially if water is already nearing lethal or avoidance levels. When considering the sites where detectable changes were observed, nearly all occurred in small catchments (< 10 km^2 and < 3 m bank full width). Numerous studies show that bull trout had a lower likelihood of occurring in small catchments with small stream widths (Dunham and Rieman 1999; Rieman and McIntyre 1995) suggesting that the streams that had greater thermal change from crossings are less likely to be used by bull trout in an undisturbed setting regardless. In one study by Dunham and Rieman (1999) they found that streams with catchments < 10 km^2 had < 10 % probability of occurrence for bull trout whereas catchments > 25 km^2 had an increased probability of occurrence to > 50 %, suggesting ecological reasons for bull trout's lack of use in smaller catchments. Similarly, westslope cutthroat trout showed an increased probability of occurrence at sites with greater stream lengths (which is correlated with stream width and catchment area, Peterson et al. 2014).

Another observation here is that not all streams had the same thermal influences and subsequently did not respond the same so findings provide some insight, but they should be considered with site specific caution. Additionally, we do not assess the cumulative impact of multiple crossings within a watershed and its effect on stream temperature so we cannot state what impacts could occur in areas with higher or lower crossing density as we did document measurable effects from some crossings in this study. Lastly, we do not explicitly state how far a measured effect lasts and this is likely site specific.

6.6 Implications for watershed management

The results of this study suggest that the thermal effects of stream crossings are minor for sites with catchment areas greater than 10 km^2 or less than 3 to 5 m bank full width. As discussed in Section 5.2, this scale-dependence likely reflects the thermal buffering effect of higher streamflow in larger catchments. This threshold is likely to vary among years, such that the threshold may be lower in a high-flow year and higher in low-flow years. As seen in Figure 7, the study period had below-average streamflow, but more extreme low-flow conditions have occurred in the historical record and may occur more commonly under future climatic conditions.

In addition to interannual variability, the threshold area for lack of thermal sensitivity to right-of-way clearing is likely to vary among regions due to both hydroclimatic and hydrogeological factors. For example, a region with frequent summer rainfall may be less sensitive due to both reduced solar radiation and higher flows due to rainfall contributions to streamflow. A region with relatively permeable bedrock that leads to strong groundwater discharge may have greater thermal buffering and, thus, a lower catchment-area threshold.

For sites with catchment areas less than 10 km^2, some right-of-way segments were thermally sensitive. If the level of sensitivity is deemed to be potentially deleterious to fish habitat quality, then some form of management intervention should be considered. The thermally sensitive streams are relatively narrow, with bankfull widths less than about 3 m. The narrowest streams could be at least partially shaded by vigorous shrub growth in the riparian zone (Gomi *et al.*, 2006). A disadvantage of relying on riparian vegetation management for shade recovery is the lag time required for vegetation to produce shade, which is a function of stream width (Quinn and Wright-Stow, 2008). An alternative to managing riparian vegetation would be to consider use of shade cloth over the stream. Johnson (2004) experimentally covered a 150-m-long reach of a 2-m-wide stream in the Oregon Cascades with black plastic and found that it reduced photosynthetically active radiation (typically about 50% of total solar radiation) above the stream by over 99% and reduced downstream warming in the reach.

6.7 Suggestions for future studies

In studies employing a replicated spatial comparison downstream design as used in the present work, there is a trade-off between the number of loggers to be installed at each site and the number of sites to be monitored. For the current study, which was intended to be completed following a single field season, the study design focused on 20 sites with four or five loggers at each site to quantify not only the temperature change within the right-of-way and an upstream reference segment, but also the downstream propagation of thermal impacts within the right-of-way. However, the information gained from loggers 4 and 5 is mostly relevant for sites at which substantial downstream warming occurs in the right-of-way. Therefore, it would be useful to conduct future studies over two field seasons. In the first season, only three loggers would be installed at each site to quantify temperature changes in each right-of-way segment and its upstream reference segment; this approach would boost the number of sites monitored in the first season. In the second season, loggers could be re-deployed from sites with minimal warming in the right-of-way segment to sites with more substantial warming to document the downstream propagation of the warming and/or to establish reference and right-of-way segments at additional sites.

A second field season could also be used to conduct more detailed studies to clarify the site factors that drive the variability in responses for sites with catchment areas less than 10 km^2 and up to 3 m in bankfull width as illustrated in Figure 27 and Figure 28. For example, more hemispherical photographs could be taken within each segment to reduce the sampling uncertainty associated with the estimated above-stream solar radiation, and further work could focus on understanding the varying role of bed heat fluxes, particularly hyporheic exchange, such as in the studies by Story *et al.* (2003) and Moore *et al.* (2005b). Another advantage of a second field season is that it would provide information on the potential for inter-annual variability and whether sites may be more thermally sensitive under future climatic conditions.

7 Conclusions and Recommendations

This study employed a replicated spatial comparison - downstream (SCD) design to evaluate the effect of forestry road crossings on stream temperature in headwater streams of the Oldman River watershed, Alberta. The study took place during the summer of 2024 and covered a range of stream sizes and crossing types. Upstream reference loggers suggested a reference warming of less than 0.4 °C in the absence of riparian disturbance. The largest effect of stream crossings was observed in maximum daily stream temperature, with daily minima responding the least. These responses were spatially variable with smaller catchment (<10 km^2) and stream sizes (< 3 m wide) being the most responsive. Responses were also likely driven by reach-scale hydrologic conditions, with hyporheic exchange influencing storage and subsequent release of heat.

Fish and fish habitat effects were not evaluated here. However, there are life stages that are supported by smaller streams for both bull trout and westslope cutthroat trout (Nelson and Paetz 1992). Studies suggest that smaller catchments have lower probabilities of bull trout and westslope cutthroat trout presence (Dunham and Rieman 1999; Peterson et al. 2014). One could interpret this as less impactful to bull trout and westslope cutthroat trout, but we do not account for downstream effects that may influence these species in areas where the probability of occurrence is higher or if many crossings exist in a catchment vs. few. It is possible that changes in thermal regimes influence these life stages and further study is required to determine these effects. A first step in this would be determining fish and invertebrate abundance within the sampled streams.

Additional field study across two years at more sites would also help in furthering the information gained through this work across more of the critical habitat along the eastern slopes of the Rocky Mountains. Future work could expand by using a lower number of loggers per site and more focused site selection on small streams.

8 Closure

MacHydro prepared this document for the account of fRI Research. The material in it reflects the judgment of MacHydro staff considering the information available to MacHydro at the time of document preparation. Any use which a third party makes of this document or any reliance on decisions to be based on is the responsibility of such third parties. MacHydro accepts no responsibility for damages, if any, suffered by any third party because of decisions made or actions based on this document.

As a mutual protection to fRI Research, the public, and ourselves, all documents are submitted for confidential information of our client for a specific project. Authorization for any use and/or publication of this document or any data, statements, conclusions, or abstracts from or regarding our documents and drawings, through any form of print or electronic media, including without limitation, posting or reproduction of same on any website, is reserved pending MacHydro's written approval. A signed and sealed copy of this document is on file at MacHydro. That copy takes precedence over any other copy or reproduction of this document.

I trust the above satisfies your requirements. Please contact us should you have any questions or comments.

Sincerely,

Ryan MacDonald Ph.D., P. Ag., Hydrologist

9 References

Albers S. 2017. Tidyhydat: Extract and tidy Canadian hydrometric data. *Journal of Statistical Software* **2**: 511 DOI: 10.21105/joss.00511

Arismendi I, Groom JD. 2019. A novel approach for examining downstream thermal responses of streams to contemporary forestry. *Science of The Total Environment* **651**: 736–748 DOI: 10.1016/j.scitotenv.2018.09.208

Aust WM, Carroll MB, Bolding MC, Dolloff CA. 2011. Operational forest stream crossings effects on water quality in the Virginia Piedmont. *Southern Journal of Applied Forestry* **35** (3): 123–130 DOI: 10.1093/sjaf/35.3.123

Behnke, R.J., and Zarn, M. 1976. Biology and management of threatened and endangered western trouts. USDA Forest Service General Tech Rep. RM 28.

Bladon KD, Cook NA, Light JT, Segura C. 2016. A catchment-scale assessment of stream temperature response to contemporary forest harvesting in the Oregon Coast Range. *Forest Ecology and Management* **379**: 153–164 DOI: 10.1016/j.foreco.2016.08.021

Bladon KD, Segura C, Cook NA, Bywater-Reyes S, Reiter M. 2018. A multicatchment analysis of headwater and downstream temperature effects from contemporary forest harvesting. *Hydrological Processes* **32** (2): 293–304 DOI: 10.1002/hyp.11415

Bonacina, L., Fasano, F., Mezzanotte, V., & Fornaroli, R. 2023. Effects of water temperature on freshwater macroinvertebrates: a systematic review. Biological Reviews, 98(1), 191-221.

Brown GW. 1969. Predicting temperatures of small streams. *Water Resources Research* **5** (1): 68–75 DOI: 10.1029/wr005i001p00068

Brown GW, Swank GW, Rothacher J. 1971. Water temperature in the Steamboat Drainage. Pacific Northwest Forest and Range Experimental Station Research Paper PNW-119. US Department of Agriculture, Forest Service, Portland, Oregon.

Caissie D, Smith A. 2022. Water temperature variability at culvert replacement sites and river thermal impacts related to the removal of an old sediment pond: application on the Barnet Brook and a tributary of the Nerepis River (New Brunswick, Canada). *Environmental Monitoring and Assessment* **194** (7) DOI: 10.1007/s10661-022-10117-5

Callahan L, Moore RD. 2025. Evaluation of the hybrid Air2stream model for simulating daily stream temperature during extreme summer heat wave and autumn drought conditions. *Hydrological Processes* **39** (1): e70033 DOI: 10.1002/hyp.70033

Chianucci F, Macek M. 2023. hemispheR: An R package for fisheye canopy image analysis. *Agricultural and Forest Meteorology* **336**: 109470 DOI: https://doi.org/10.1016/j.agrformet.2023.109470

Coats WA, Jackson CR. 2020. Riparian canopy openings on mountain streams: Landscape controls upon temperature increases within openings and cooling downstream. *Hydrological Processes* **34** (8): 1966–1980 DOI: 10.1002/hyp.13706

COSEWIC. 2016. *COSEWIC assessment and status report on the Westslope Cutthroat Trout Oncorhynchus clarkii Lewis, Saskatchewan-Nelson River populations and Pacific populations in Canada*. Committee on the Status of Endangered Wildlife in Canada.

Cunningham DS, Braun DC, Moore JW, Martens AM. 2023. Forestry influences on salmonid habitat in the North Thompson River watershed, British Columbia. *Canadian Journal of Fisheries and Aquatic Sciences* DOI: 10.1139/cjfas-2022-0255

Dent L, Vick D, Abraham K, Schoenholtz S, Johnson S. 2008. Summer temperature patterns in headwater streams of the Oregon Coast Range. *JAWRA Journal of the American Water Resources Association* **44** (4): 803–813 DOI: 10.1111/j.1752-1688.2008.00204.x

Diebel MW, Fedora M, Cogswell S, O'Hanley JR. 2015. Effects of road crossings on habitat connectivity for stream-resident fish. *River Research and Applications* **31** (10): 1251–1261 DOI: https://doi.org/10.1002/rra.2822

Dunham, J.B. and Rieman, B.E., 1999. Metapopulation structure of bull trout: influences of physical, biotic, and geometrical landscape characteristics. Ecological Applications, 9(2), pp.642-655.

Dunham, J., Rieman, B. and Chandler, G., 2003. Influences of temperature and environmental variables on the distribution of bull trout within streams at the southern margin of its range. North American Journal of Fisheries Management, 23(3), pp.894-904.

Dunham JB, Rosenberger AE, Luce CH, Rieman BE. 2007. Influences of wildfire and channel reorganization on spatial and temporal variation in stream temperature and the distribution of fish and amphibians. *Ecosystems* **10** (2): 335–346 DOI: 10.1007/s10021-007-9029-8

Erbs DG, Klein SA, Duffie JA. 1982. Estimation of the diffuse radiation fraction for hourly, daily and monthly-average global radiation. *Solar Energy* **28** (4): 293–302 DOI: 10.1016/0038-092x(82)90302-4

Fisheries and Oceans Canada. 2020b. *Recovery strategy for the bull trout (salvelinus confluentus), saskatchewan-nelson rivers populations, in canada [proposed]. Species at risk act recovery strategy series*. Fisheries; Oceans Canada.

Fisheries and Oceans Canada. 2020a. *Recovery strategy for the rainbow trout (oncorhynchus mykiss) in canada (athabasca river populations) [proposed]. Species at risk act recovery strategy series*. Fisheries; Oceans Canada.

Gomi T, Moore RD, Dhakal AS. 2006. Headwater stream temperature response to clear-cut harvesting with different riparian treatments, coastal British Columbia, Canada. *Water Resources Research* **42** (8) DOI: 10.1029/2005wr004162

Groom JD, Dent L, Madsen LJ, Fleuret J. 2011. Response of western Oregon (USA) stream temperatures to contemporary forest management. *Forest Ecology and Management* **262** (8): 1618–1629 DOI: 10.1016/j.foreco.2011.07.012

Guenther SM, Gomi T, Moore RD. 2014. Stream and bed temperature variability in a coastal headwater catchment: influences of surface-subsurface interactions and partial-retention forest harvesting. *Hydrological Processes* **28** (3): 1238–1249 DOI: 10.1002/hyp.9673

Heckel IV, J. W., Quist, M. C., Watkins, C. J., & Dux, A. M. 2020. Distribution and abundance of Westslope Cutthroat Trout in relation to habitat characteristics at multiple spatial scales. North American Journal of Fisheries Management, 40(4), 893-909.

Herunter HE, Macdonald JS, MacIsaac EA. 2003. Influence of logging road right-of-way size on small stream water temperature and sediment infiltration in the Interior of B.C. In *Forestry Impacts on Fish Habitat in the Northern Interior of British Columbia: A Compendium of Research from the Stuart-Takla Fish-Forestry Interaction Study. Canadian Technical Report on Fisheries and Aquatic Science 2509*, MacIsaac EA (ed.).Fisheries and Oceans Canada, Science Branch, Pacific Region; 223–238.

Hunt LM, Arlinghaus R, Lester N, Kushneriuk R. 2011. The effects of regional angling effort, angler behavior, and harvesting efficiency on landscape patterns of overfishing. *Ecological Applications* **21** (7): 2555–2575 DOI: https://doi.org/10.1890/10-1237.1

Isaak DJ, Luce CH, Rieman BE, Nagel DE, Peterson EE, Horan DL, Parkes S, Chandler GL. 2010. Effects of climate change and wildfire on stream temperatures and salmonid thermal habitat in a mountain river network. *Ecological Applications* **20**: 1350–1371 DOI: 10.1890/09-0822.1

Isaak DJ, Wollrab S, Horan D, Chandler G. 2012. Climate change effects on stream and river temperatures across the northwest u.s. From 1980–2009 and implications for salmonid fishes. *Climatic Change* **113**: 499–524 DOI: 10.1007/s10584-011-0326-z

Isaak, D.J. and Young, M.K., 2023. Cold-water habitats, climate refugia, and their utility for conserving salmonid fishes. Canadian Journal of Fisheries and Aquatic Sciences, 80(7), pp.1187-1206.

Janisch JE, Wondzell SM, Ehinger WJ. 2012. Headwater stream temperature: Interpreting response after logging, with and without riparian buffers, Washington, USA. *Forest Ecology and Management* **270**: 302–313 DOI: 10.1016/j.foreco.2011.12.035

Johnson SL. 2004. Factors influencing stream temperatures in small streams: substrate effects and a shading experiment. *Canadian Journal of Fisheries and Aquatic Sciences* **61** (6): 913–923 DOI: 10.1139/f04-040

Kemp P, Sear D, Collins A, Naden P, Jones I. 2011. The impacts of fine sediment on riverine fish. *Hydrological Processes* **25** (11): 1800–1821 DOI: https://doi.org/10.1002/hyp.7940

Leach JA, Moore RD. 2010. Above-stream microclimate and stream surface energy exchanges in a wildfire-disturbed riparian zone. *Hydrological Processes* **24**: 2369–2381 DOI: 10.1002/hyp.7639

Leach JA, Hudson DT, Moore RD. 2022. Assessing stream temperature response and recovery for different harvesting systems in northern hardwood forests using 40 years of spot measurements. *Hydrological Processes* **36** (11) DOI: 10.1002/hyp.14753

Lynch JA, Rishel GB, Corbett ES. 1984. Thermal alteration of streams draining clearcut watersheds: Quantification and biological implications. *Hydrobiologia* **111** (3): 161–169 DOI: 10.1007/bf00007195

Macnaughton, C.J., Durhack, T.C., Mochnacz, N.J. and Enders, E.C., 2021. Metabolic performance and thermal preference of Westslope cutthroat trout (Oncorhynchus clarkii lewisi) and non-native trout across an ecologically relevant range of temperatures1. Canadian Journal of Fisheries and Aquatic Sciences, 78(9), pp.1247-1256.

McIntyre, J., and Rieman, B. 1995. Westslope Cutthroat Trout. In Conserva-tion Assessment for Inland Cutthroat Trout. Edited by M. Young. Tech.Report RM-GTR-256. USDA Forest Service

Moore RD, MacDonald RJ. 2024. Quantifying the influence of forestry and forest disturbance on stream temperature: Methodologies and challenges. *Hydrological Processes* **38** (7) DOI: 10.1002/hyp.15223

Moore RD, Guenther SM, Gomi T, Leach JA. 2023. Headwater stream temperature response to forest harvesting: Do lower flows cause greater warming? *Hydrological Processes* **37**: e15025 DOI: 10.1002/hyp.15025

Moore RD, Richards G, Story A. 2008. Electrical conductivity as an indicator of water chemistry and hydrologic process. *Streamline Watershed Management Bulletin* **11** (2): 25–29 Available at: http://library.nrs.gov.bc.ca/digipub/Streamline.V11N02.pdf

Moore RD, Spittlehouse DL, Story A. 2005a. Riparian microclimate and stream temperature response to forest harvesting: a review. *Journal of the American Water Resources Association* **41** (4): 813–834 DOI: 10.1111/j.1752-1688.2005.tb04465.x

Moore RD, Sutherland P, Gomi T, Dhakal A. 2005b. Thermal regime of a headwater stream within a clear-cut, coastal British Columbia, Canada. *Hydrological Processes* **19** (13): 2591–2608 DOI: 10.1002/hyp.5733

Naiman, R. J., & Decamps, H. 1997. The ecology of interfaces: riparian zones. Annual review of Ecology and Systematics, 28(1), 621-658.

Nelitz MA, MacIsaac EA, Peterman RM. 2007. A science-based approach for identifying temperature-sensitive streams for Rainbow Trout. *North American Journal of Fisheries Management* **27** (2): 405–424 DOI: 10.1577/m05-146.1

Nelson JS, Paetz MJ. 1992. *The fishes of alberta*. University of Alberta.

Oanh D, Gomi T, Moore RD, Chiu C-W, Hiraoka M, Onda Y, Dung B. 2021. Stream temperature response to 50% strip-thinning in a temperate forested headwater catchment. *Water* **13**: 1022 Available at: http://dx.doi.org/10.22541/au.160337371.12604694/v1

Park D, Sullivan M, Bayne E, Scrimgeour G. 2008. Landscape-level stream fragmentation caused by hanging culverts along roads in alberta's boreal forest. *Canadian Journal of Forest Research* **38** (3): 566–575 DOI: 10.1139/X07-179

Peterson, D.P., Rieman, B.E., Horan, D.L. and Young, M.K., 2014. Patch size but not short-term isolation influences occurrence of westslope cutthroat trout above human-made barriers. Ecology of Freshwater Fish, 23(4), pp.556-571.

Quinn JM, Wright-Stow AE. 2008. Stream size influences stream temperature impacts and recovery rates after clearfell logging. *Forest Ecology and Management* **256** (12): 2101–2109 DOI: 10.1016/j.foreco.2008.07.041

Raulerson S, Jackson CR, Melear ND, Younger SE, Dudley M, Elliott KJ. 2020. Do southern Appalachian Mountain summer stream temperatures respond to removal of understory rhododendron thickets? *Hydrological Processes* **34** (14): 3045–3060 DOI: 10.1002/hyp.13788

Rex JF, Maloney DA, Krauskopf PN, Beaudry PG, Beaudry LJ. 2012. Variable-retention riparian harvesting effects on riparian air and water temperature of sub-boreal headwater streams in British Columbia. *Forest Ecology and Management* **269**: 259–270 DOI: 10.1016/j.foreco.2011.12.023

Rieman, B. E., and J. D. McIntyre. 1995. Occurrence of bull trout in naturally fragmented habitat patches of varied size. Transactions of the American Fisheries Society 124:285– 296.

Selong, J.H., McMahon, T.E., Zale, A.V. and Barrows, F.T., 2001. Effect of temperature on growth and survival of bull trout, with application of an improved method for determining thermal tolerance in fishes. Transactions of the American fisheries Society, 130(6), pp.1026-1037.

Sievert C. 2020. Interactive web-based data visualization with R, plotly, and shiny Available at: https://plotly-r.com
Sowder C, Steel EA. 2012. A note on the collection and cleaning of water temperature data. *Water* **4** (3): 597–606 DOI: 10.3390/w4030597
Story A, Moore RD, Macdonald JS. 2003. Stream temperatures in two shaded reaches below cutblocks and logging roads: downstream cooling linked to subsurface hydrology. *Canadian Journal of Forest Research* **33** (8): 1383–1396 DOI: 10.1139/x03-087
Tabacchi E, Lambs L, Guilloy H, Planty-Tabacchi A-M, Muller E, Décamps H. 2000. Impacts of riparian vegetation on hydrological processes. *Hydrological Processes* **14** (16-17): 2959–2976 DOI: https://doi.org/10.1002/1099-1085(200011/12)14:16/17<2959::AID-HYP129>3.0.CO;2-B
Webb BW, Hannah DM, Moore RD, Brown LE, Nobilis F. 2008. Recent advances in stream and river temperature research. *Hydrological Processes* **22** (7): 902–918 DOI: 10.1002/hyp.6994

10 Appendix A – Time series plots of stream temperature for each site

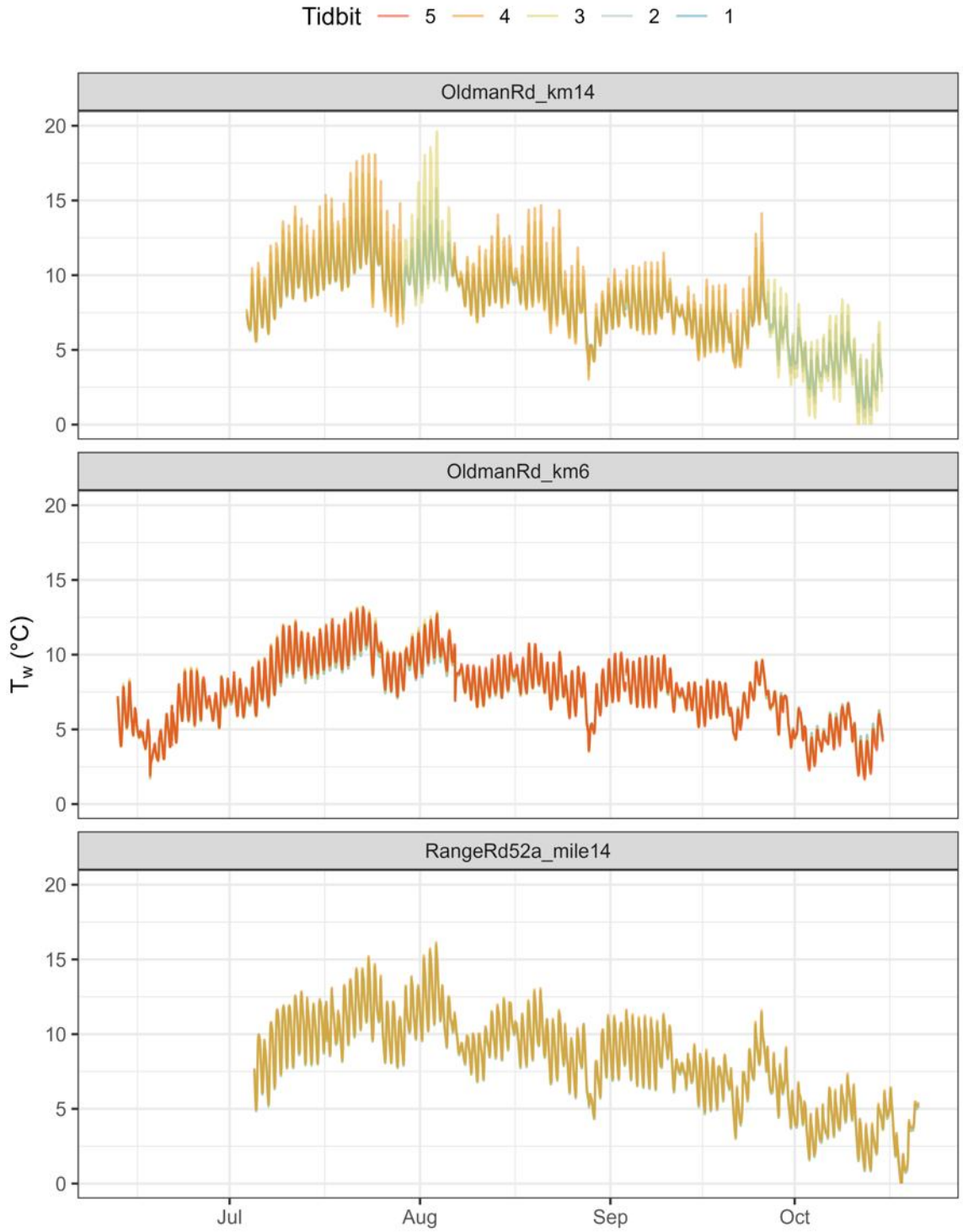

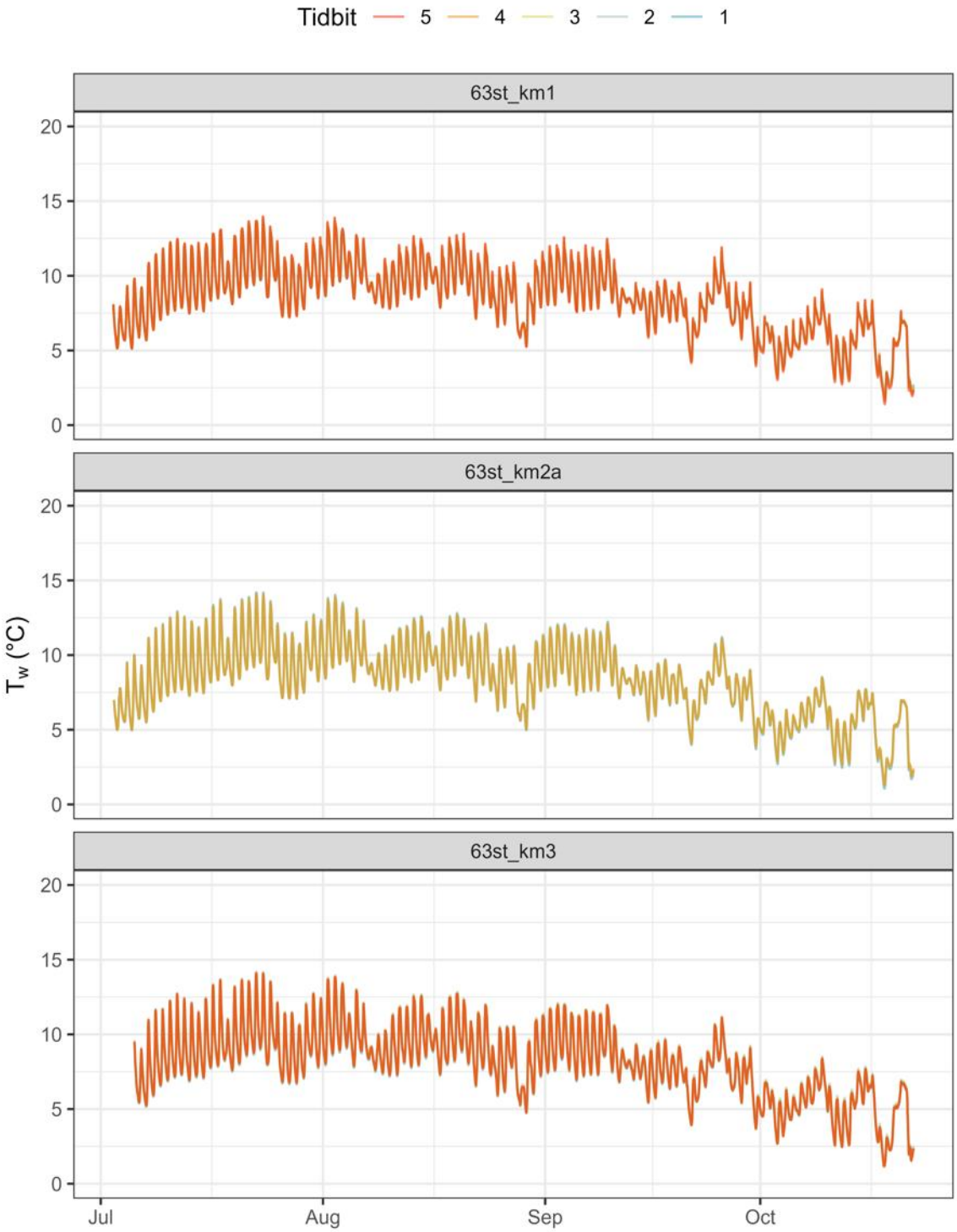
Tidbit 5 4 3 2 1
63st_km1
63st_km2a
63st_km3
T_w (°C)
0
5
10
15
20
Jul
Aug
Sep
Oct

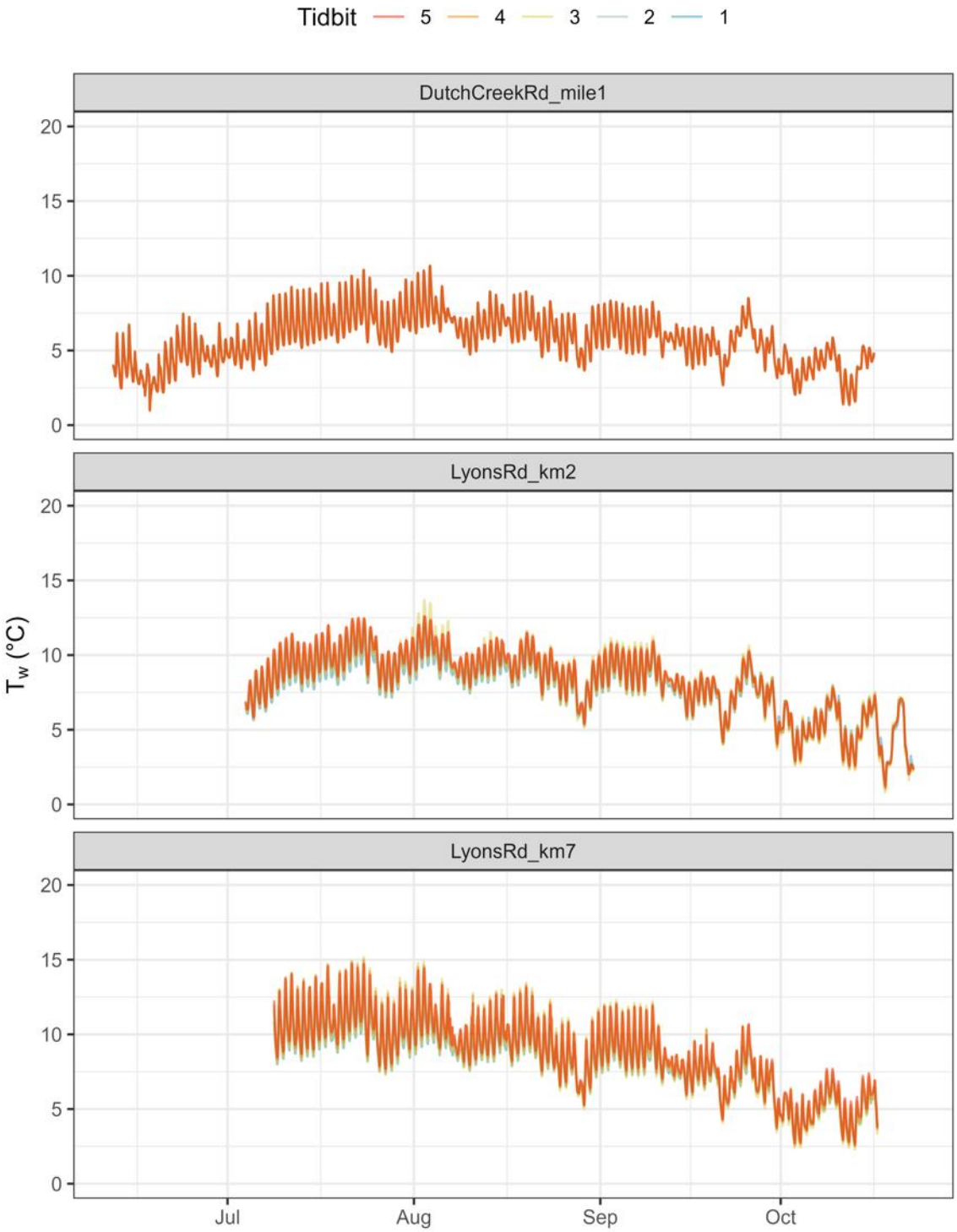
Tidbit 5 4 3 2 1
DutchCreekRd_mile1
LyonsRd_km2
LyonsRd_km7
T_w (°C)
0
5
10
15
20
Jul
Aug
Sep
Oct

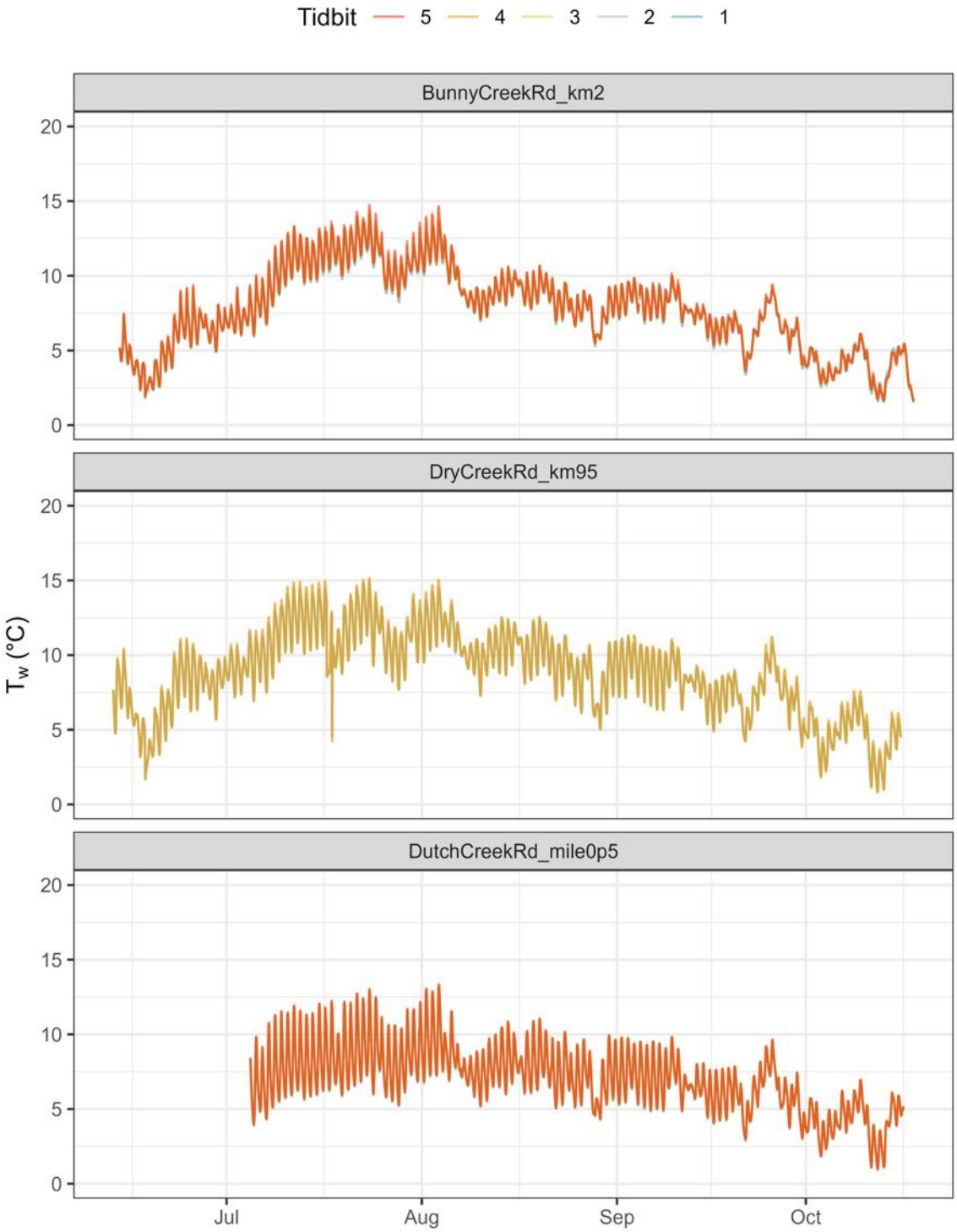
Tidbit 5 4 3 2 1
BunnyCreekRd_km2
DryCreekRd_km95
DutchCreekRd_mile0p5
T_w (°C)
0
5
10
15
20
Jul
Aug
Sep
Oct

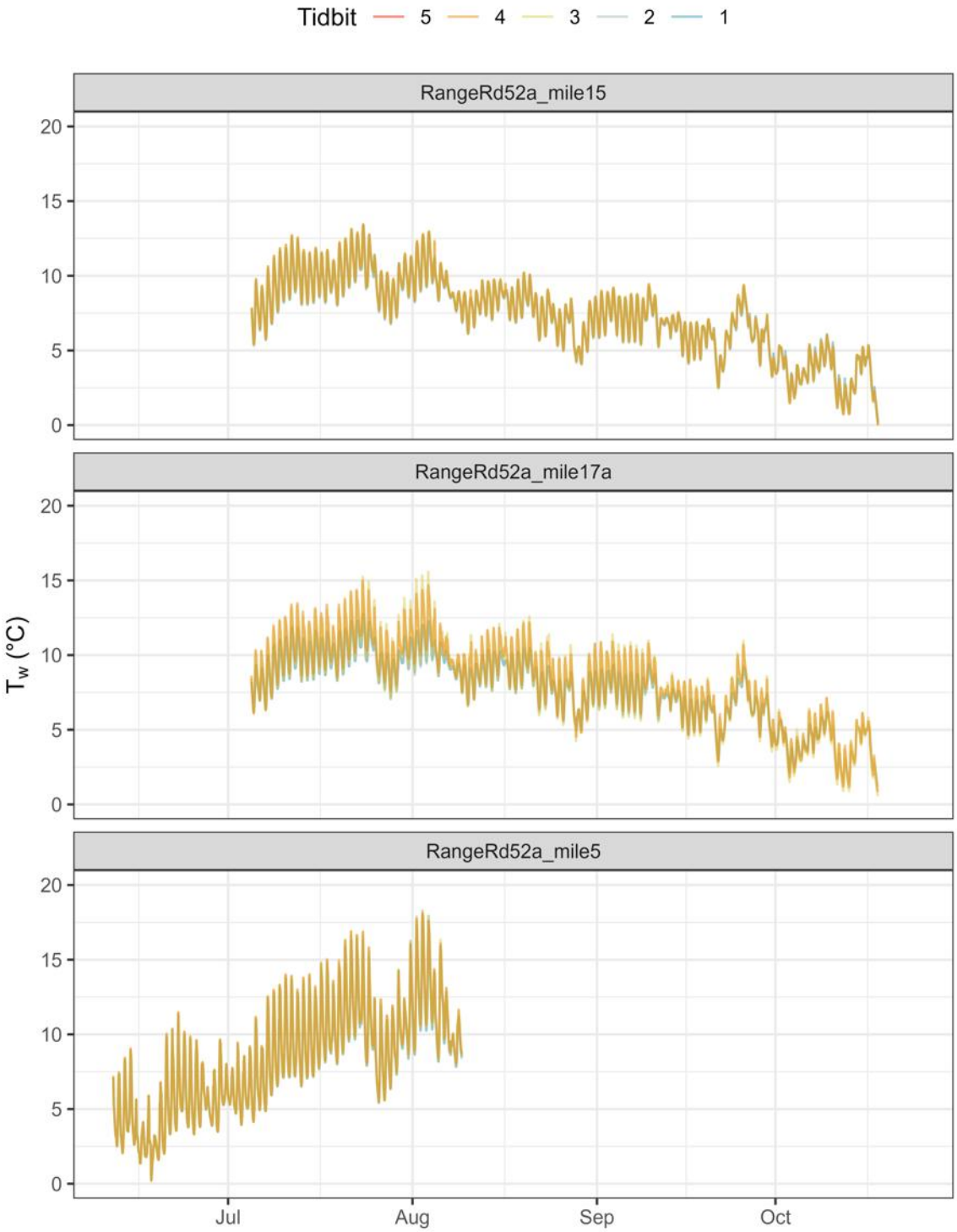
Tidbit 5 4 3 2 1
RangeRd52a_mile15
RangeRd52a_mile17a
RangeRd52a_mile5
T_w (°C)
0
5
10
15
20
Jul
Aug
Sep
Oct

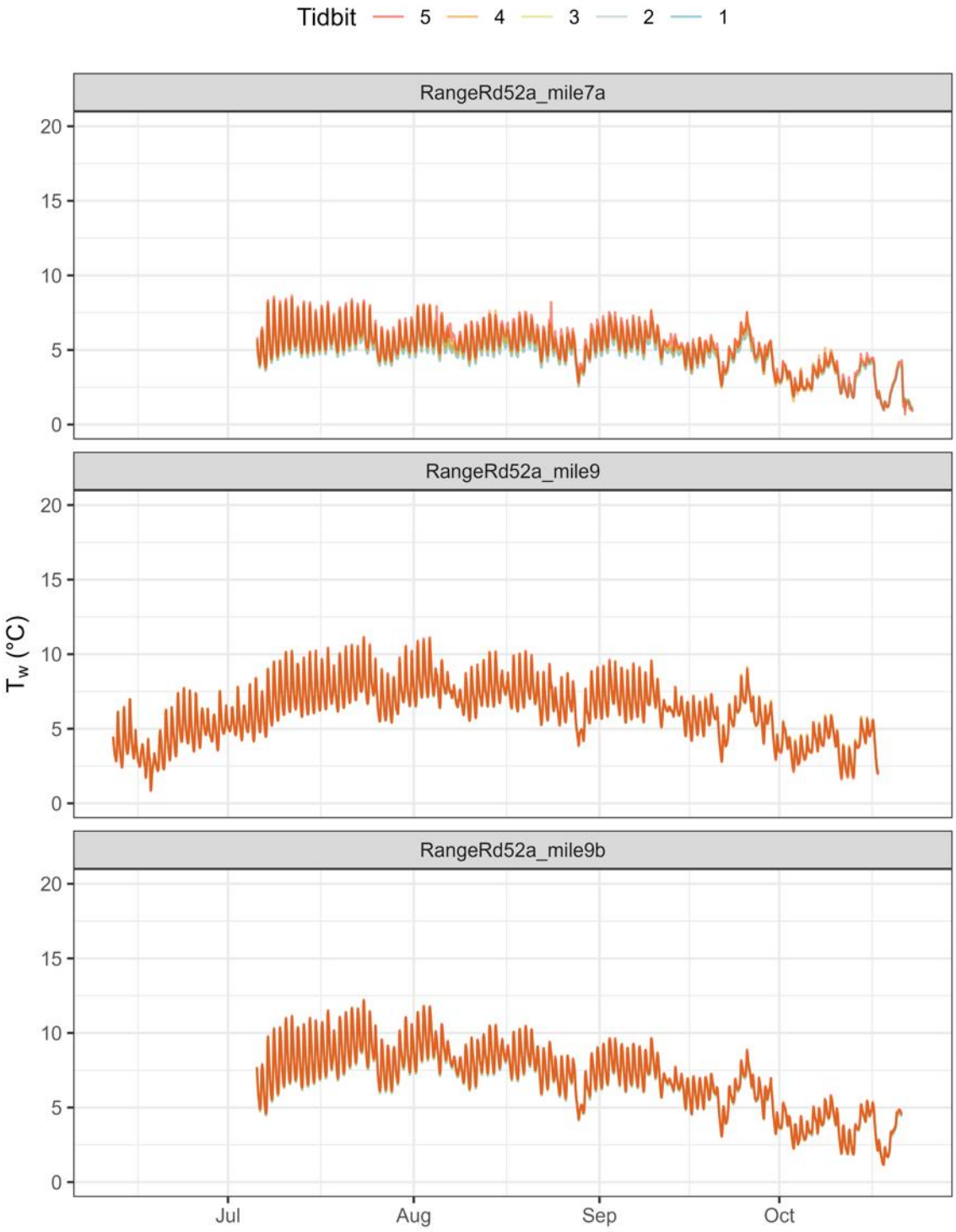
Tidbit 5 4 3 2 1
RangeRd52a_mile7a
RangeRd52a_mile9
RangeRd52a_mile9b
T_w (°C)
0
5
10
15
20
Jul
Aug
Sep
Oct